



저작자표시-비영리-변경금지 2.0 대한민국

이용자는 아래의 조건을 따르는 경우에 한하여 자유롭게

- 이 저작물을 복제, 배포, 전송, 전시, 공연 및 방송할 수 있습니다.

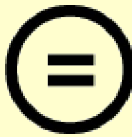
다음과 같은 조건을 따라야 합니다:



저작자표시. 귀하는 원저작자를 표시하여야 합니다.



비영리. 귀하는 이 저작물을 영리 목적으로 이용할 수 없습니다.



변경금지. 귀하는 이 저작물을 개작, 변형 또는 가공할 수 없습니다.

- 귀하는, 이 저작물의 재이용이나 배포의 경우, 이 저작물에 적용된 이용허락조건을 명확하게 나타내어야 합니다.
- 저작권자로부터 별도의 허가를 받으면 이러한 조건들은 적용되지 않습니다.

저작권법에 따른 이용자의 권리는 위의 내용에 의하여 영향을 받지 않습니다.

이것은 [이용허락규약\(Legal Code\)](#)을 이해하기 쉽게 요약한 것입니다.

[Disclaimer](#)

Thesis for the Degree of Master of Science

A length-based assessment model for the common squid

(*Todarodes pacificus*) population

caught by multiple fisheries in Korean waters



by

Min Gyou Park

Department of Marine Biology

The Graduate School

Pukyong National University

February 2021

A length-based assessment model for the common squid
(*Todarodes pacificus*) population
caught by multiple fisheries in Korean waters
[체장기반모델을 이용하여 복수어업에서 어획되는
한국 살오징어 (*Todarodes pacificus*) 자원평가]

Advisor: Prof. Saang-Yoon Hyun

By
Min Gyou Park

A thesis submitted in partial fulfillment of the requirements
for the degree of

Master of Science

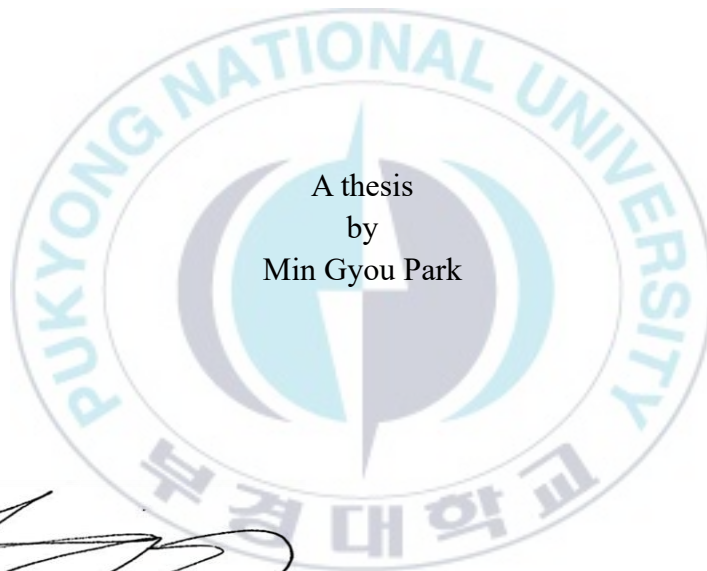
in Department of Marine Biology, The Graduate School,
Pukyong National University

February 2021

A length-based assessment model for the common squid

(*Todarodes pacificus*) population

caught by multiple fisheries in Korean waters



A thesis
by
Min Gyou Park

Approved by:

A handwritten signature in black ink, appearing to be "Jin Koo Kim", written over a horizontal line.

(Chairman) Dr. Jin Koo Kim

A handwritten signature in black ink, appearing to be "Yeonghye Kim", written over a horizontal line.

(Member) Dr. Yeonghye Kim

A handwritten signature in black ink, appearing to be "Saang-Yoon Hyun", written over a horizontal line.

(Member) Dr. Saang -Yoon Hyun

February 19, 2021

Contents

List of figures.....	iii
List of tables.....	viii
요 약.....	xi
I. A length-based assessment model for the common squid (<i>Todarodes pacificus</i>) population caught by multiple fisheries in Korean waters	1
1. Introduction.....	1
2. Materials and Methods	5
2.1. Data.....	5
2.2. Length-based model	7
2.3. Parameter estimation	26
2.4. Model performance	30
3. Results	34
3.1. Assessment for the common squid	34
3.2. Model performance	54
4. Discussion.....	60

II. How should we randomly sample marine fish landed at Korean ports to estimate the length frequency distribution of those fish?.....	68
1. Introduction.....	68
2. Methods	72
2.1. Simulated length composition data.....	72
2.2. Inference of parameters	75
2.3. Simulation experiments	79
3. Results	83
4. Discussion.....	97
Conclusions.....	99
Acknowledgements.....	100
References.....	101
Appendix 1. Derivation of expected length and variance of aged individual.	107
Appendix 2. TMB code for the length-based assessment model for the common squid.....	111

List of figures

- Fig. 2.1 Fitted fecundity at length $\hat{\phi}(x)$ from the length-fecundity data (Kim et al., 1997). The points denote data, and the solid line denotes the fitted line ($\phi(x) = \hat{\eta}_0 \cdot x^{\hat{\eta}_1} = 6.5 \cdot 10^{-3} \cdot x^{4.86}$). The vertical axis denotes the number of eggs ($\times 10^5$) and the horizontal axis denotes mantle length in cm..... 39
- Fig. 2.2. Bimonthly yield data, Y_t^g , of the common squid from the three fisheries in Korea and the predicted yield for each fishery Y_t^g from the length-based model. The solid line denotes the predicted yield from the model, and the points denote the observed yield data. The vertical axis denotes yield in MT ($\times 10^4$) and the horizontal axis denotes time (bimonth). Panel (a), (b), and (c) are jigger, large purse-seine, and the others, respectively..... 41
- Fig. 2.3. Predicted length frequency of jigger fishery from length-based model and observed Length composition data from May and June 2016 to November and December 2018. The horizontal axis denotes length classes with width of 1 cm and the vertical axis

denotes frequencies at each length class. The histograms denote the observed data, and the solid lines denote predicted values. 43

Fig. 2.4. Predicted length frequency of large purse-seine fishery from length-based model and observed length composition data from May and June 2016 to November and December 2018. The horizontal axis denotes length classes with a width of 1cm and the vertical axis denotes the frequencies of each length class. The histograms denote the observed data, and the solid lines denote predicted values. 45

Fig. 2.5. Predicted weight at length $W(x)$ from the length-based model. Gray points denote observed data (1,091 squid), and the solid line denotes the predicted value ($W(x) = \hat{\alpha} \cdot x^{\hat{\beta}} = 0.06 \cdot x^{2.7}$). The horizontal axis denotes mantle length in cm, and the vertical axis denotes body weight in grams. 46

Fig. 2.6. Predicted bimonthly recruitment from May and June 2016 to November and December 2018, and projected recruitment in January and February 2019 of the common squid stock. The vertical axis denotes recruitment in number ($\times 10^{10}$) and the horizontal axis denotes time (bimonth). 47

Fig. 2.7. Predicted bimonthly biomass from May and June 2016 to November and December 2018 and projected biomass in January and February 2019 of the common squid stock. Solid line denotes the predicted biomass of the common squid stock, the dotted line denotes the predicted biomass of mature males, dash-dotted line denotes the predicted biomass of mature females, and dashed line denotes the predicted biomass of spawners. The vertical axis denotes biomass in MT ($\times 10^5$) and the horizontal axis denotes time (bimonth). 48

Fig. 2.8. Predicted size-specific natural mortality rate $M(x)$. The vertical axis denotes instantaneous natural mortality rate (bimonth^{-1}) and the horizontal axis denotes length class in cm. 49

Fig. 2.9. Predicted bimonthly instantaneous fishing mortality rates of (a) jigger, (b) large purse-seine, and (c) the other fisheries. The vertical axis denotes instantaneous fishing mortality (bimonth^{-1}) and the horizontal axis denotes time (bimonth). 51

Fig. 2.10. Predicted probability mass functions (PMF) of length distribution by age of the cohort recruited in May and June 2016. Solid lines denote the predicted PMF of a cohort ($f_{t,a}(x)$), dotted line denotes the predicted PMF of a cohort of males ($f_{t,a}^{\delta}(x)$), and

the dashed line denotes the predicted PMF of a cohort of females ($f_{t,a}^{\dagger}(x)$). Panels are separated by time and age of the cohort: (a) t = May and June 2016, and $a = 1$; (a) t = July and August 2016, and $a = 2$; (a) t = September and October 2016, and $a = 3$; (a) t = November and December 2016, and $a = 4$; (a) t = January and February 2017, $a = 5$; (a) t = March and April 2017, and $a = 6+ \dots$ 53

Fig. 2.11. Box plots of relative differences (RDs) of estimates for each level of measurement error. Scenarios $CV_{10\%}$, $CV_{30\%}$, and $CV_{50\%}$, are the measurement errors in all yield data sets with 10%, 30%, and 50% levels of coefficient of variation. Boxes represent the interquartile range (25th – 75th percentile). Bold lines in the boxes indicate the median value of RDs , and lines outside the whiskers indicate the upper and lower fences..... 59

Fig. 3.1. Process of arranging fish landed..... 71

Fig. 3.2. Comparison in estimates ($\hat{\pi}$) of composition between the current and alternative practices with a sample size of 200 under four scenarios when a total of all fish landed (C) was 0.1 million individuals. The first row shows the length frequency of fish landed set under each scenario. The second and third rows are the results of current and alternative practices, respectively. Open

circles are true compositions and points (-) are the mean values of estimates by length class and the vertical bars are the standard deviations of estimates from 1,000 replicates..... 92

Fig. 3.3. Comparison in estimates ($\hat{\pi}$) of composition between the current and alternative practices with a sample size of 200 under four scenarios when a total of all fish landed (C) was 1 million individuals. The first row shows the length frequency of fish landed set under each scenario. The second and third rows are results from current and alternative practices, respectively. Open circles are true compositions and points (-) are the mean values of estimates by length class and the vertical bars are the standard deviations of estimates from 1,000 replicates..... 94

Fig. 3.4. Boxplots of 95% coverage probabilities of estimates of length compositions (i.e., 40 $\hat{\pi}$'s in the multinomial likelihood) by sample size considered. Simulation was performed for each of 10 cases of sample size (100, 200, ..., 1,000) under four scenarios by two cases of a total of fish landed ($C = 0.1$ million individuals under the left column; $C = 1$ million individuals under the right column). Gray boxes denote the current sampling practice while blank boxes represent the alternative sampling practice..... 96

List of tables

Table 2.1. List of symbols and their definitions used in the length-based assessment model.....	21
Table 2.2. Estimates of 35 free parameters and standard of error (SE) of the estimates in actual data sets.	32
Table 2.3. Parameter values assigned to the length-based assessment model for the common squid, including growth (μ_r , L_∞), length-maturation (β_0 , β_1), natural mortality (b_1), length-fecundity (η_0 , η_1), and female ratio at recruitment ($\chi_{t,r}^\ddagger$) parameters. μ_r , L_∞ , β_0 , β_1 , and b_1 are taken from previous studies (Sakurai et al., 2013; Jo et al., 2019; Lorenzen, 1996). η_0 and η_1 are taken from the additional estimation with length-fecundity data.....	38
Table 2.4. Mean value of residual sum of squares (RSS) of six variables constituting the likelihood function under different levels of measurement error scenarios from 1,000 replicates. In the scenarios, $CV_{10\%}$, $CV_{30\%}$, and $CV_{50\%}$ indicate the measurement error in all data sets with 10%, 30%, and 50% levels of coefficient of	

variation. Scenario ‘Actual data’ refers to the actual data sets, and is shown for comparison with the simulation experiments..... 57

Table 3.1. List of symbols. Values used in the simulation are under “Setting values”..... 76

Table 3.2. Simulation scenarios of the length distribution of a population (i.e., a total of fish landed). Length distributions of all fish landed were generated under four scenarios with the assumption that the total of all fish landed was 0.1 and 1 million, respectively. μ and σ are the mean and the standard deviation of a truncated normal distribution. The shape of a length distribution differs by scenario: (1) S1: skewed to the right; (2) S2: symmetrical; (3) S3: skewed to the left; (4) S4: uniform. 82

Table 3.3. Sampling weights used by the current practice (w_h^{Current}) versus those used by the alternative practice (w_h^{Proposal}) set under each scenario when a total of all fish landed (C) was assumed to be 0.1 million. Five size groups are divided as follows: VSG: very small size group, (10cm, 18cm]; SG: small size group, (18cm, 26cm]; MG: medium size group, (26cm, 34cm]; LG: large size group, (34cm, 42cm]; VLG: very large group, (42cm, 50cm]..... 85

Table 3.4. Sampling weights used by the current practice (w_h^{Current})

versus those used by the alternative practice (w_h^{Proposal}) set under each scenario when a total of all fish landed (C) was assumed to be 1 million. Five size groups are divided as follows: VSG: very small size group, (10cm, 18cm]; SG: small size group, (18cm, 26cm]; MG: medium size group, (26cm, 34cm]; LG: large size group, (34cm, 42cm]; VLG: very large group, (42cm, 50cm]..... 88



A length-based assessment model for the common squid
(*Todarodes pacificus*) population caught by multiple fisheries
in Korean waters

박 민 규

부경대학교 대학원 해양생물학과

요 약

오랫동안 두족류의 자원평가는 독특한 생물학적인 특성 (e.g, 산란, 회유, 성장, 등) 과 자료 수집의 어려움에 의하여 어려운 과제였다 (Fries, 2010). 한국과 일본 해역에 분포하는 살오징어 (*Todarodes pacificus*)는 상업적인 가치가 높은 두족류로서 (Nakamura, 1993; Kidokoro et al., 2010), 한국해역에서 약 25개의 어업에서 어획이 되고 있는 실정이다. 이러한 상황에서, 본 연구는 살오징어의 생물학적 특성, 자료 수집의 어려움, 그리고 복수 어업 환경을 반영한 자원평가 모델의 필요성을 동기로서, 체장조성자료 (length composition data)를 이용하는 Quinn et al. (1998)의 체장기반모델 (length-based model)을 바탕으로 한국 해역에 분포하고 있는 살오징어 개체군에 특화된 자원평가 모델을 개발하였고, 가상실험 (simulation-estimation experiment)을 수행하여 모델의 추정 성능 (Estimability)을 확인하였다. 모델의 중점 개선사항은 다음과 같다: (i) 복수어업을 고려하기 위해, 어업별 체장조성자료의 사용가능성에 따라 어업

을 구분하였다; (ii) 살오징어의 체성장을 설명하기 위해, Gompertz 성장 모델을 사용하였다; (iii) 순간 자연사망률을 개체의 체장에 대한 함수로서 나타냈다; (iv) 모든 코호트는 암수로 구분되었으며, 암수 성별간 서로 다른 생식 (reproduction)에 의한 사망이 가정되었다; (v) 체장별 포란수에 대한 정보를 사용하여, 산란-가입 관계식 (spawner-recruitment relationship)을 적용하였다. 가상실험의 결과로서, 모델은 Gompertz 성장식에 관련된 모수의 추정에는 문제가 발견되지 않았으나, 산란과 사망률에 관련된 모수의 추정에 문제를 나타냈다. 본 연구에서는 모델의 핵심자료인 체장조성자료의 수집 과정에 대한 추가적인 조사를 수행하였다. 한국에서의 체장조성자료는 어획물이 체급별로 분류되어 상자에 담기는 배열 (arrangement)이라는 과정을 거친 후 수집되는데, 현행 표집 방법은 체급별로 분류된 상자수에 비례하여 체급별 표본을 추출하는 것이다. 본 연구에서는 현행 표집 방법으로 얻어지는 체장조성자료가 총 어획물의 체장 조성을 대표할 수 있는지를 확인하기 위해, 배열 과정과 현행 표집을 재현한 가상실험을 수행하여 평가하였고, 체급별 어획물의 수에 비례하여 체급별로 표본을 수집할 때, 총 어획물의 체장 조성을 대표할 수 있음을 밝혔다. 따라서, 본 논문은 체장기반 살오징어 자원평가 모델에 대한 연구와 체장조성자료의 수집방법의 제안이라는 두가지의 연구를 다루었으며, 각 연구는 두개의 장 (chapter)으로 구분되어 서술되었다: I. A length-based assessment model for the common squid (*Todarodes pacificus*) population caught by multiple fisheries in Korean waters; II. How should we randomly sample marine fish landed at Korean ports to estimate the length frequency distribution of those fish?.

I. A length-based assessment model for the common squid (*Todarodes pacificus*) population caught by multiple fisheries in Korean waters

1. Introduction

Fishery stock assessments can be performed using any of a wide variety of assessment models. The selection of a specific model for a stock assessment is tailored to the available data and, in general, a less detailed model is chosen when fewer data are available (NOAA, 2020). Biomass dynamics models, such as the surplus production model, the most basic approach, are virtually the only method used in situations where the only data available are a time series of catches and some index of abundance (Punt 2003). Age-structured models, such as statistical catch-at-age models, which are dominant in contemporary stock assessment, require an index of population size, such as a survey index or a measure of catch-per-unit-effort, the total catch from fisheries, and composition data specific to individual age classes. These models are able to assess the population dynamics more accurately than surplus production models, because they reconstruct population data and trace temporal changes in a cohort, using

information about the age composition of a population (Punt et al., 2013). However, the applicability of these models is limited by difficulties in collecting age composition data, arising from considerations of factors such as cost, expertise, and time required. Considering these circumstances, size- (or length-) based models are adequate alternatives to age-structured models. An advantage of length-based models over age-structured models is that all processes can be size-based, and these processes can modify the size-at-age distribution (Punt et al., 2013).

The length-based model has developed from that described by Cohen and Fishman (1980), Deriso and Parma (1988), and Quinn et al. (1998). Cohen and Fishman (1980) developed a stochastic growth model representing the body growth process of a cohort over time, incorporating stochastic error using a von Bertalanffy growth model. Deriso and Parma (1988) utilized the stochastic growth model from Cohen and Fishman (1980), and included recruitment, growth, natural mortality, gear selectivity, and fishing mortality into a length-based model. Quinn et al. (1998) converted the length distribution to a discrete distribution. I developed a length-based assessment model based on that of Quinn et al. (1998), and applied the model to stock of the common squid (*Todarodes pacificus*) in Korean waters. My extensions of their model are based on the biology of the common squid, and the specific characteristics of

fisheries in Korean waters.

The common squid is a commercially important species in Korea, and is exploited by about 25 fisheries. There are no fisheries whose yield comprises half of the total yield of the fisheries. Common squid are short-lived, surviving for only about a year. During its lifespan, the squid hatch and migrate northward from the spawning ground. They feed and grow for seven to eight months, and then migrate southward to the spawning ground, where they reproduce (Sakurai et al., 2013; Kim et al., 2011). Spawning occurs throughout the year. This stock is separated into three subpopulations according to peak spawning season: winter from January to April; summer from May to August; and autumn from September to December. The subpopulations exhibit different biomass and body growth (Sakurai et al., 2013; Kim et al., 2011).

My model incorporates five major new features. First, according to the availability of the length composition data, I separated the 25 fisheries of common squid into jigger, large purse-seine, and others, to reflect the use of multiple technologies in fisheries in Korean waters. Second, I applied the Gompertz growth model instead of the von Bertalanffy model of the body growth of the common squid, because the Gompertz growth model more accurately explains the body growth of the common squid, which exhibits low growth rates in early life (Sakurai et al., 2013;

Sugawara et al., 2013). Third, I estimated the parameters of the allometric relationship of natural mortality to individual body size, using an approach modified from Lorenzen (1996), in which natural mortality varies according to individual body mass. Fourth, recruitment in my model was linked to the spawners, using fecundity information as an alternative way of building a stock-recruitment model, such as the Beverton-Holt or Ricker models. Fifth, all cohorts were divided into males and females, to enable modelling of the differences in the reproductive mortality between males and females, and to incorporate the female capacity for laying eggs.

In this chapter, I present two studies: (i) a length-based assessment model for the Korea common squid; and (ii) a simulation-estimation experiment to evaluate the model performance.

2. Materials and Methods

2.1. Data

Five types of data were used in the model: (i) length-composition; (ii) catch-per-unit-effort (CPUE); (iii) commercial yield; (iv) length-weight; and (v) length-fecundity data.

The length data, as measured by mantle length, of the common squid caught from jigger (JIG) and large purse-seine (PS) fisheries from May 2016 to December 2018 were provided by the Korean National Institute of Fisheries Science (NIFS). The length data were transformed into length-composition data by discretizing the data into 34 length classes. Each class is 1 cm wide, and is defined by the midpoint of the class. For example, a class label of 0.5 cm therefore indicates membership of the class of squid whose mantle length is in the range [0cm, 1cm). Because the length-composition data has many missing monthly values, the model takes two months to be one discrete time step. Thus, length composition data were aggregated bimonthly.

The monthly CPUE data from JIG and PS fisheries from May 2016 to December 2018 were provided by the NIFS. Because two months comprised one time step, the CPUE data were modified by dividing the sample yield (MT) for two months by sample fishing effort (hooks for JIG;

hauls for PS) for two months.

The bimonthly total yield for the common squid from JIG, PS, and the other (TO) fisheries were provided by Statistics Korea (KOSTAT). The yield from PS fisheries in July and August 2018 was revised from 1100.23 MT, representing the sum of frozen fish (687.266 MT) and fresh fish (412.964 MT) to 412.964 MT, including only fresh fish. Since PS fisheries in Korea use a carrier transporting fresh fish to a port, frozen fish (687.266 MT) in July and August 2018 is unusual.

The mantle length and body weight of 1,091 squid were measured by NIFS and myself. Kim et al. (1997) demonstrated a length-fecundity relationship of female common squid by measuring the mantle length and the number of eggs laid by individuals (Kim et al., 1997). These data are currently not available, so the length-fecundity data were obtained by scanning Figure 4 of the publication by Kim et al. (1997) using the 'Engauge Digitizer' (Mark et al., 2020) software.

2.2. Length-based model

All symbols used are summarized in Table 2.1. The age of each cohort is assumed to be in increments of two months from recruiting age $r=1$ to the terminal age $A=6+$. Age r was set to two months after birth, and age A was set to 6+, 12 months or more after birth, under the assumption that some individuals could survive more than 12 months. In a recruited cohort ($N_{t,r}$), the abundance of recruiting age r at the beginning of time t is classified by sex by multiplying the sex ratio at recruitment:

$$N_{t,r}^y = N_{t,r} \cdot \chi_{t,r}^y, \quad (1)$$

where superscript $y \in \{\♂, ♀\}$ (male, female) and $\chi_{t,r}^y$ is the proportion of sex y at recruitment. The lengths of recruitment for each sex (X_r^y) are discrete variables, which are normally distributed with mean μ_r and variance σ_r^2 (i.e., $X_r^y \sim Normal_D[\mu_r, \sigma_r^2]$). The probability mass function (PMF) of X_r^y for the length class x at the beginning of time t can be denoted as:

$$f_{i,r}^y(x) = \varphi\left(\frac{x - \mu_r}{\sigma_r}\right) / \sum_x \varphi\left(\frac{x - \mu_r}{\sigma_r}\right), \quad (2)$$

where function φ is the probability density function (PDF) of a standard normal distribution. Thus, the abundance of recruited males and females at each length class is $N_{i,r}^y(x) = N_{i,r}^y \cdot f_{i,r}^y(x)$.

The dynamics of a cohort is assumed to be compounded of mortality and body growth processes over time, from age r to terminal age A . Following Deriso and Parma (1988), the process of mortality took place first, then body growth occurs.

The total mortality rate, $Z_t(x)$, is obtained by summing the natural mortality rate and the mortality rate for each fishery, g , where $g \in \{J, P, TO\}$ (JIG, PS, TO):

$$Z_t(x) = M(x) + \sum_g F_t^g(x). \quad (3)$$

Lorenzen (1996) modelled natural mortality rate as a power function of weight, accounting for the relationship between natural mortality and body weight for different aquaculture systems, as well as species and families,

$M(W) = b_0 \cdot W^{-b_1}$. In my model, natural mortality rate is modified from Lorenzen (1996), varying by length class through the allometric length-weight relationship, $W(x) = \alpha \cdot x^\beta$:

$$M(x) = b_0 \cdot [W(x)]^{-b_1} . \quad (4)$$

For each fishery, time- and size-specific fishing mortality rate $F_t^g(x)$ is the product of bimonthly fully-selected fishing mortality rate and size-specific gear selectivity:

$$F_t^g(x) = F_t^g \cdot S^g(x) . \quad (5)$$

The fully-selected fishing mortality rate for JIG and PS are assumed to be proportionate to fishing effort, while a time-series random walk model was assumed for TO:

$$F_t^g = \begin{cases} q^g \cdot \text{Effort}_t^g & \text{for } g = J \text{ or } P \\ F_{t-1}^g \cdot \exp[\delta_{t-1}] & \text{for } g = TO \end{cases}, \quad (6)$$

for $g = J$ or P , catchability q^g is assumed to be a time-invariant constant and Effort_t^g is calculated by dividing yield by the corresponding CPUE.

For $g = TO$, δ_{t-1} , the deviation term of log-scaled time-series fishing mortality rate is assumed to follow a normal distribution with mean 0 and variance σ_δ^2 (i.e., $\delta_{t-1} \sim N[0, \sigma_\delta^2]$). The reason why F_t^{TO} was treated as time-series random walk model is that fishing effort data for TO are not available. Size-specific gear selectivity for JIG and PS is based on a logistic form as a function of length class, while gear selectivity for TO is not assumed, due to the absence of length composition data:

$$S^g(x) = \frac{1}{1 + \exp(-\gamma^g \cdot (x - L_{50\%}^g))} \quad \text{for } g = J \text{ or } P \quad (7)$$

where $L_{50\%}^g$ is the length at which half of the stock encountered in

fisheries are captured, and γ^s is a shape parameter that determines the steepness of the selectivity curve.

Based on the life history of the common squid (SeaLifeBase, 2020), it is assumed that each sex of the common squid undergoes an additional mortality process due to reproduction. For males, it is assumed that mature individuals can participate in reproduction and then die. For females, even if the individual matures, it is assumed that only a mature individual who arrives at the spawning ground can participate in reproduction and then die. Thus, mature males and post-spawning females have died in this model.

The age- and size-specific rate participation in reproduction is assumed to differ by sex:

$$\psi_a^y(x) = \begin{cases} \pi_a \cdot Mat(x) & \text{for } y = \text{♀} \\ Mat(x) & \text{for } y = \text{♂} \end{cases} . \quad (8)$$

For females, $\psi_a^{\text{♀}}(x)$ is the product of the size-specific maturation, $Mat(x)$, and the age-specific arrival rate at the spawning ground, π_a .

For males, $\psi_a^\delta(x)$ is the age-independent, size-specific maturation. Since the common squid begins its spawning migration at seven to eight months after birth (Kim et al., 2011), the age-specific arrival rate at the spawning ground is assumed to start from age five (i.e., 10 months old): $\pi_a = (0, 0, 0, 0, \pi_5, 1)$. The size-specific maturation is based on a logistic form (Jo et al., 2019):

$$Mat(x) = \frac{1}{1 + \exp[\beta_0 + \beta_1 \cdot x]} \quad (9)$$

Given the PMF of the length distribution of both male and female at the beginning of time t at age a , the relative distribution of lengths at the end of time t after the mortality process is:

$$p_{t,a,z}^y(x) = f_{t,a}^y(x) \cdot \exp(-Z_t(x)) \cdot (1 - \psi_a^y(x)) \quad (10)$$

The process of body growth is based on the assumption that an individual of length class x will grow to length class l during one time step,

according to the stochastic Gompertz growth model. The deterministic Gompertz growth model is:

$$L_a = L_\infty \cdot \exp\left[-\exp(-G \cdot (a - a_0))\right],$$

where L_∞ is the asymptotic length, and G is the instantaneous growth rate at age a_0 , and a_0 is the age at the inflection point of the curve (Tjørve et al., 2017).

The formula for size L_{a+1} at age $a+1$ was derived as a function of the previous size, L_a , at age a , with the multiplicative error term from the deterministic Gompertz growth model.

$$L_{a+1} = L_\infty \cdot \left(\frac{L_a}{L_\infty}\right)^\rho \cdot e^{\varepsilon_G} ; \varepsilon_G \sim N(0, \sigma_G^2)$$

where $\rho = \exp[-G]$ and the error term ε_G is assumed to be normally distributed with mean zero and variance σ_G^2 . I also derived the expected lengths and variance at age $a+1$ for an individual of the length class x at

age a , using a method from Cohen and Fishman (1980) (Appendix 1):

$$\mu_G(x) = L_\infty \cdot \left(\frac{x}{L_\infty} \right)^\rho \cdot \exp \left[\frac{\sigma_G^2}{2} \right] \quad (11)$$

and

$$\sigma_{a+1}^2 = \exp \left[2 \cdot (E(\log L_{a+1}) + \text{Var}(\log L_{a+1})) \right] - \exp \left[2 \cdot E(\log L_{a+1}) + \text{Var}(\log L_{a+1}) \right] \quad (12)$$

The length of an individual at age $a+1$ originated from length class x at age a is a discrete random variable, which is normally distributed with mean $\mu_G(x)$ and variance σ_{a+1}^2 , $L | x \sim \text{Normal}_D[\mu_G(x), \sigma_{a+1}^2]$.

Thus, the PMF for the length distribution at $a+1$ originated from length class x at age a is given by

$$f_{a+1,G}(l|x) = \varphi \left(\frac{l - \mu_G(x)}{\sigma_{a+1}} \right) / \sum_l \varphi \left(\frac{l - \mu_G(x)}{\sigma_{a+1}} \right). \quad (13)$$

After mortality and growth over a bimonth, the relative distribution of lengths for each sex at age $a+1$ at the beginning of time $t+1$ is given by:

$$p_{t+1,a+1}^y(l) = \sum_x p_{t,a,z}^y(x) \cdot f_{a+1,G}(l|x). \quad (14)$$

For each sex, the number of individuals in length class l at age $a+1$ at the beginning of time $t+1$ and corresponding PMF of the length distribution are then

$$N_{t+1,a+1}^y(l) = N_{t,a}^y \cdot p_{t+1,a+1}^y(l), \quad (15)$$

and

$$f_{t+1,a+1}^y(l) = p_{t+1,a+1}^y(l) / \sum_l p_{t+1,a+1}^y(l). \quad (16)$$

The number of spawners in length class l at age $a+1$ at the beginning of time $t+1$ is obtained from equation (8) and (15):

$$\text{SSN}_{t+1,a+1}(l) = N_{t+1,a+1}^{\dagger}(l) \cdot \psi_{a+1}^{\dagger}(l). \quad (17)$$

The recruitment at the beginning of time $t+1$ is assumed to be linked to the number of eggs at the beginning of time t through fecundity. The number of eggs at time t is given by

$$\text{Egg}_t = \sum_x \sum_a \text{SSN}_{t,a}(x) \cdot \phi(x), \quad (18)$$

where $\phi(x)$ is the size-specific fecundity, and is modelled as the allometric relationship to the individual size of mature females, $\phi(x) = \eta_0 \cdot x^{\eta_1}$. Then, the recruitment at the beginning of time $t+1$ is

$$N_{t+1,r} = \text{Egg}_t \cdot \exp[-M(0.5\text{cm})], \quad (19)$$

where $M(0.5\text{cm})$ is the natural mortality for the first length class (0.5 cm). The length of individuals at hatching is assumed to be in the range from

0.0 cm to 1.0 cm, based on a previous study indicating that paralarval mantle lengths of the common squid measured 0.95mm at hatching (Sakurai et al., 2013).

For time $t >$ initial time (t_{init}), the number of individuals at length class x of age a at the beginning of time t is given as:

$$N_{t,a}(x) = \begin{cases} \sum_y N_{t,a}^y \cdot f_{t,a}^y(x) & \text{for } a = r \\ \sum_y N_{t-1,a-1}^y \cdot p_{t,a}^y(x) & \text{for } r < a < A \\ \sum_y [N_{t-1,a-1}^y \cdot p_{t,a}^y(x) + N_{t-1,a}^y \cdot p_{t,A}^y(x)] & \text{for } a = A \end{cases} \quad (20)$$

for $a = A$, $\sum_y N_{t-1,a}^y \cdot p_{t,A}^y(x)$ is the individuals of age A surviving at time $t-1$ (i.e., abundance at age $A+1$ at the time t), as described by Millar and Hyun (2018). However, the number of individuals at length class x of age a at time t_{init} is given as:

$$N_{t_{init},a}(x) = \sum_y N_{t_{init},a}^y \cdot f_{t_{init},a}^y(x) \cdot \chi_{t_{init},a}^y, \quad (21)$$

where $f_{t_{init},a}^y(x)$ and $\chi_{t_{init},a}^y$ are the PMF of the length distribution and the sex ratio of sex y at age a at time t_{init} , respectively. The calculation of $f_{t_{init},a}^y(x)$ and $\chi_{t_{init},a}^y$ follows the assumptions: (1) length of recruitment is normally distributed, with mean μ_r and variance σ_r^2 ; (2) sex ratio of sex y at age r is the same as at other times; (3) only reproduction is considered in the mortality process; (4) body growth is modelled according to a the stochastic Gompertz growth model. Thus, $f_{t_{init},a}^y(l)$ and $\chi_{t_{init},a}^y$ are given as

$$f_{t_{init},a}^y(l) = \frac{p_{t_{init},a}^y(l)}{\sum_l p_{t_{init},a}^y(l)} \quad (22)$$

and

$$\chi_{t_{init},a}^y = \frac{\sum_l p_{t_{init},a}^y(l)}{\sum_l \sum_y p_{t_{init},a}^y(l)}, \quad (23)$$

where $p_{t_{mit},a}^y(l)$ is the relative length distribution of sex y at age a at time t_{mit} and is the same concept as equation (14):

$$p_{t_{mit},a}^y(l) = \begin{cases} \varphi\left(\frac{l-\mu_r}{\sigma_r}\right) / \sum_l \varphi\left(\frac{l-\mu_r}{\sigma_r}\right) & \text{for } a = r \\ \sum_x p_{t_{mit},a-1}^y(x) \cdot (1-\psi_{a-1}^y(x)) \cdot f_{a,G}(l|x) & \text{for } 1 < a \leq A \end{cases} \quad (24)$$

To obtain the number of common squid caught at length class x by fishery g during time t , I used the continuous catch formulation, as proposed by Baranov (1945), which assumes that fishing mortality and natural mortality occur simultaneously during each time step (Branch, 2009). Fishing mortality and natural mortality are proportional to abundance and work simultaneously and uniformly throughout one time step. Thus, the number of common squid caught of length class x by fishery g during the time t is given by

$$C_t^g(x) = \sum_a N_{t,a}(x) \cdot \frac{F_t^g(x)}{Z_t(x)} \cdot (1 - e^{-Z_t(x)}). \quad (25)$$

The biomass and yield of each fishery were obtained from the size-specific abundance and catch of each fishery by multiplying the allometric length-weight relationship, as follows:

$$B_t(x) = \sum_a N_{t,a}(x) \cdot W(x),$$
$$Y_t^g(x) = C_t^g(x) \cdot W(x).$$
(26)

The total biomass and yield of each fishery during the time t is given as:

$$B_t = \sum_x B_t(x),$$
$$Y_t^g = \sum_x Y_t^g(x).$$
(27)

Table 2.1. List of symbols and their definitions used in the length-based assessment model.

Symbol	Description
a	Age
A	Terminal age, age 6+ considered (i.e., 12 months).
b_0, b_1	Parameters in allometric length-fecundity relationship
B_t	Total biomass of population at the beginning of time t
$B_t(x)$	Biomass of population at the beginning of time t of length class x
$C_t^g(x)$	Individuals at length class x caught by fishery g during time t
$CPUE_t^g$	Catch-per-unit-effort data collected from fishery g in time t
CV_Y^g	Coefficient of variance of lognormal distribution for yield of fishery g : $CV_Y^g = \sqrt{\exp[(\sigma_Y^g)^2] - 1}$
CV_δ	Coefficient of variance of lognormal distribution for fishing mortality of the other fishery: $CV_\delta = \sqrt{\exp[\sigma_\delta^2] - 1}$
Effort $_t^g$	Fishing effort of fishery g in time t : Effort $_t^g = Y_t^g / CPUE_t^g$
Egg $_t$	Number of eggs at the beginning of time t

$f_{a+1,G}(l x)$	Conditional probability of individuals at the length class (l) after one growth increment for an individual at the length class (x)
$f_{t,a}^y(x)$	Probability of individuals at the length class x of a cohort, with sex y and age a at the beginning of time t
F_t^g	Instantaneous fishing mortality rate of fishery g at time t
g	Fisheries
G	Instantaneous growth rate
ℓ	Log-likelihood function
L	A length class after one growth increment
L_a	Length at age a
$L_{50\%}^g$	Length of fish when the fish encountered the fishery g is caught with 50% probability
L_∞	Asymptotic length
m_t^g	The exploited length composition of fishery g at time t
$\text{Mat}(x)$	Maturation at length class x
$M(x)$	Instantaneous natural mortality rate at length class x
n_t^g	Number of samples of length composition data from fishery g in year t
$N_{t,a}(x)$	Number of individuals at length class x of age a at the beginning of time t

$N_{t,a}^y(x)$	Number of individuals at length class x of sex y at age $a+1$ at the beginning of time t
$\hat{\delta}_t^g(x)$	Predicted proportion of model catch at length class x during time t
<i>Obj</i>	The objective function
$p_{t+1,a+1}^y(l)$	Relative distribution of lengths of a cohort at age a of sex y at the beginning of time t after the processes of mortality and growth
$p_{t,a,z}^y(x)$	Relative distribution of lengths of a cohort at age a of sex y at the end of time t after the process of mortality
q^g	Catchability coefficient of fishery g
r	Recruitment age, age $r = 1$
R_t	Number of individuals of age r at the beginning of time t
$SSN_{t,a}(x)$	Number of spawners at length class l of age a at the beginning of time t
$S^g(x)$	Size-specific gear selectivity for fishery g
t	Time, defined as a bimonth
t_{init}	Time at the beginning of May and June 2016
$W(x)$	Body weight of length class x
$\hat{W}(x)$	Predicted body weight of length class x
x	Length class before one growth increment
X_r	Discrete random variable which measures length of

	recruitment
Y_t^g	Yield from fishery g in time t
\hat{Y}_t^g	Predicted yield from fishery g in time t
$Z_t(x)$	Total mortality rate at length class x in time t
α, β	Parameters in allometric length-weight relationship
β_0, β_1	Parameters in maturation
γ^g	Shape parameter in gear selectivity of fishery g
δ_t	Deviation of log-scaled fishing mortality rate for the other fishery
η_0, η_1	Parameters in allometric length-fecundity relationship
λ_1, λ_2	Weighting terms for the length composition data
λ_3	Weighting terms for the length-weight data
μ_r	Mean length of a recruitment
$\mu_G(x)$	Expected length after growth increment for an individual of the length class x
ρ	$\exp(-G)$
π_5	Arrival rate at spawning ground of a cohort of age 5
σ_{a+1}^2	Variance of the length distribution at age $a+1$ after

	growth for an individual of the length class x at age a
σ_{δ}^2	Variance of normal distribution for δ_t
σ_G^2	Variance of stochastic error term in the Gompertz growth equation
σ_r^2	Variance of length distribution of a recruitment
σ_W^2	Variance of $W(x)$
σ_Y^g	Standard deviation of $\log Y_t^g$
$\phi(x)$	Fecundity at mantle length
$\varphi(\cdot)$	Probability density function of standard normal distribution
$\chi_{t,a}^y$	Sex ratio of sex y at age a at the beginning of time t
$\psi_a^y(x)$	Size- and age-specific reproductive rate for each sex

2.3. Parameter estimation

I constructed six independent random vectors for extracting information about parameters from each data set using a likelihood principle. The exploited length composition of JIG and PS at time t (m_t^J, m_t^P) are assumed to be distributed as multinomial distribution:

$$m_t^g \sim \text{multinomial}(n_t^g, \hat{\theta}_t^g).$$

where n_t^g is the sample size of the length composition data at time t by fishery g , and $\hat{\theta}_t^g(x)$ is the predicted proportion of a length class x in my length-based model catch (equation (25)).

$$\hat{\theta}_t^g(x) = \frac{\hat{C}_t^g(x)}{\sum_x \hat{C}_t^g(x)}$$

The yields of three fisheries during the time t are assumed to be lognormally distributed:

$$Y_t^g = \hat{Y}_t^g \cdot \exp[\varepsilon_Y^g]; \quad \varepsilon_Y^g \sim N\left[0, (\sigma_Y^g)^2\right]$$

$$Y_t^g \sim \text{lognormal}\left[\hat{Y}_t^g, (\sigma_Y^g)^2\right]$$

where \hat{Y}_t^g is model yield of fishery g at time t (equation (27)), and $(\sigma_Y^g)^2$ is the variance of $\log Y_t^g$. The weight at length ($W(x)$) is assumed to be distributed according to a normal distribution:

$$W(x) = W(x) + \varepsilon_w; \quad \varepsilon_w \sim N\left[0, \sigma_w^2\right]$$

$$W(x) \sim N\left[W(x), \sigma_w^2\right]$$

where $W(x)$ is the predicted value for fitting length-weight data and σ_w^2 is the variance of $W(x)$. I also included a lognormal penalty to control the degree of variability in the time series of F_t^{TO} estimates (Fu et al, 2000),

$$F_t^{TO} = F_{t-1}^{TO} \cdot \exp[\delta_{t-1}]; \quad \delta_{t-1} \sim N\left[0, \sigma_\delta^2\right]$$

$$F_t^{TO} \sim \text{lognormal}\left[F_{t-1}^{TO}, \sigma_\delta^2\right]$$

Thus, I constructed objective function (*Obj*) composed of six log-likelihood components and one penalized likelihood component:

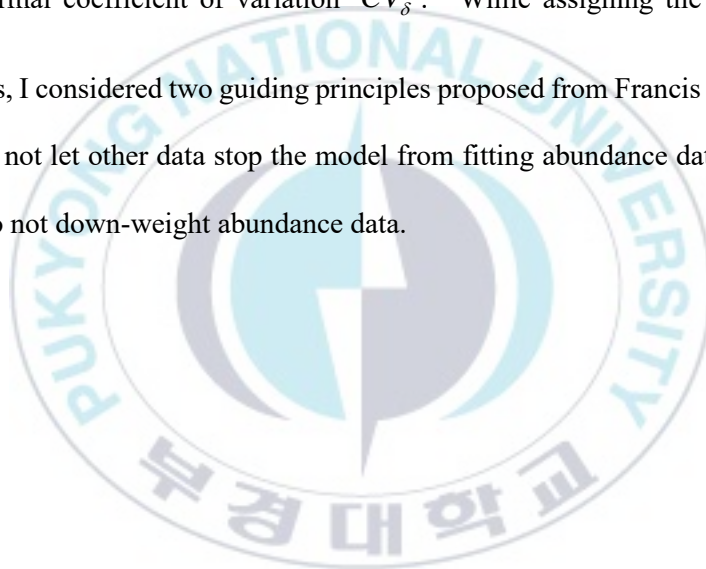
$$Obj = -\lambda_1 \cdot \ell(\boldsymbol{\theta} | \mathbf{m}^J) - \lambda_2 \cdot \ell(\boldsymbol{\theta} | \mathbf{m}^P) - \ell(\boldsymbol{\theta} | \mathbf{Y}^J, CV^J) - \ell(\boldsymbol{\theta} | \mathbf{Y}^P, CV^P) - \ell(\boldsymbol{\theta} | \mathbf{Y}^{TO}, CV^{TO}) - \lambda_3 \cdot \ell(\boldsymbol{\theta} | \mathbf{W}) - \ell(\boldsymbol{\theta} | \mathbf{F}^{TO}, CV_\delta) \quad (28)$$

where λ_1 , λ_2 , λ_3 , CV_Y^J , CV_Y^P , and CV_Y^{TO} are weighting terms and coefficients of variations (i.e., $CV_Y^s = \sqrt{\exp[(\sigma_Y^s)^2] - 1}$) for corresponding likelihood functions, and are assigned to each data set. The last term $\ell(\boldsymbol{\theta} | \mathbf{F}^{TO}, CV_\delta)$ is a penalized likelihood function, and CV_δ was assigned to control the variability of F_t^{TO} estimates. A large value of CV_δ makes the bimonthly fishing mortality of TO very small.

The parameters were estimated using the TMB (Kristensen et al. 2016) package in R (R Core Team 2020) software. The TMB script (code for length-based assessment model) is shown in the Appendix 2. I used the “nlminb” function in R for parameter estimation via minimizing the objective function value. The point estimates were obtained by

numerically differentiating Obj with respect to the free parameters, and the standard errors of the estimates were obtained by the delta method.

With the data from common squid stock, the values 0.004, 0.005, 0.05, 80 %, 53 %, and 112 % were assigned to the weight parameters λ_1 , λ_2 , λ_3 , CV_Y^J , CV_Y^P , and CV_Y^{TO} . The value 30% was assigned to the lognormal coefficient of variation CV_δ . While assigning the weight values, I considered two guiding principles proposed from Francis (2011):
(i) do not let other data stop the model from fitting abundance data well;
(ii) do not down-weight abundance data.



2.4. Model performance

I performed a simulation-estimation experiment to evaluate model performance with respect to the robustness and estimability of parameters under different measurement error (ME) circumstance. Values of parameters for constructing simulated data were taken from estimates of actual data (Table 2.2). I also included uncertainties in the process of fishing mortality rate of TO (\mathbf{F}^{TO}), to generate simulated data. Thus, the \mathbf{F}^{TO} were generated by imposing a lognormal error with CV of 10% upon a random walk model.

To evaluate the model according to the level of the ME, three scenarios were used for the ME in the yield data sets from each fishery. In each scenario, the ME in the yield data were assigned as being the same type and level (i.e., lognormal errors with $CV_Y^J = CV_Y^P = CV_Y^{TO}$). The levels of the ME in the three scenarios were 10, 30, and 50%. Thus, the simulated yield data for each fishery were generated as lognormal random values by imposing a lognormal error with a CV for each scenario. The simulated length composition data for JIG and PS were generated as multinomial random values, by imposing a multinomial error with an effective sample size of 1,000. However, the length-weight data for each scenario were used as actual data.

For each scenario, simulated data corresponding to random fishing mortality of TO were generated and input into the length-based assessment model, which iterated 1,000 times. Then, the estimates from each iteration were calculated in the form of relative difference (*RD*) to estimate the bias for each scenario (Miller and Hyun, 2018). The *RD* of parameter estimate θ_i from the true value θ for *i*-th iterations is given as

$$RD_i(\theta) = \frac{\theta - \theta_i}{|\theta_i|} .$$

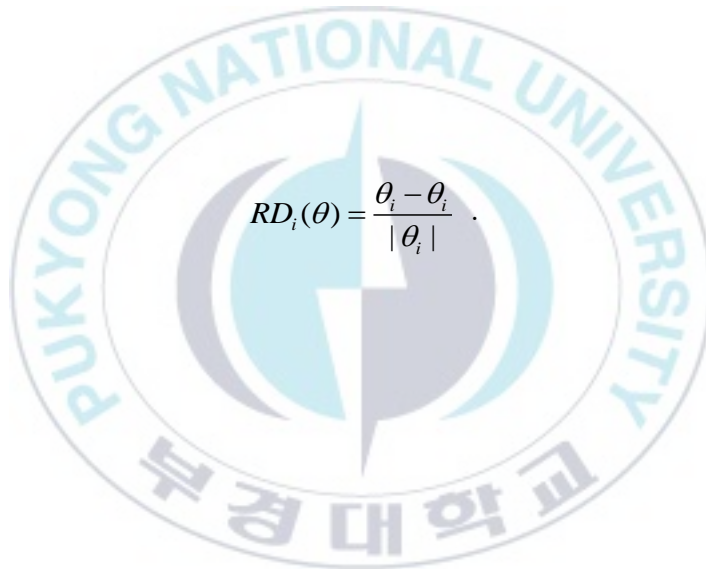
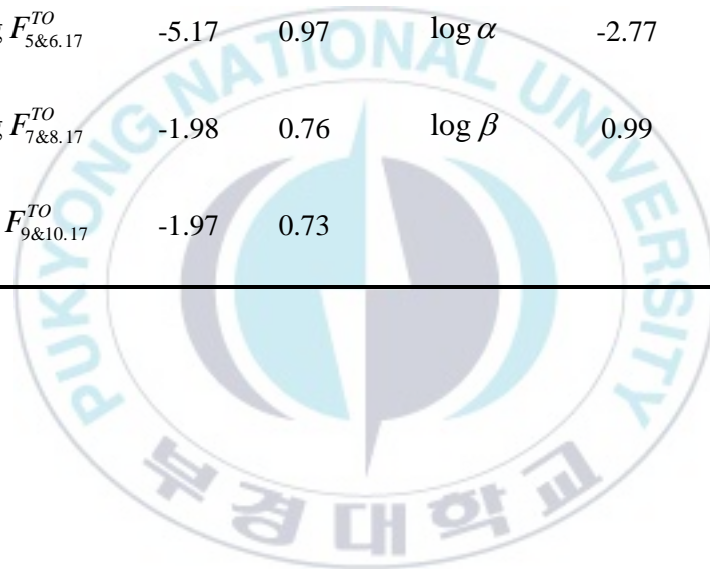


Table 2.2. Estimates of 35 free parameters and standard of error (SE) of the estimates in actual data sets.

Parameters	Estimates	SE	Parameters	Estimates	SE
$\log \sigma_r^2$	-1.91	0.36	$\log F_{11\&12.17}^{TO}$	-1.93	0.75
$\log G$	-0.72	0.02	$\log F_{1\&2.18}^{TO}$	-1.96	0.77
$\log \sigma_G$	-7.16	1.13	$\log F_{3\&4.18}^{TO}$	-5.39	0.90
$\log q^J$	-14.91	0.87	$\log F_{5\&6.18}^{TO}$	-5.36	0.90
$\log q^P$	-12.92	0.88	$\log F_{7\&8.18}^{TO}$	-0.97	0.90
γ^J	0.91	0.41	$\log F_{9\&10.18}^{TO}$	-0.96	0.88
γ^P	0.78	0.22	$\log F_{11\&12.18}^{TO}$	-0.98	0.90
$\log L_{50\%}^J$	2.89	0.07	$\log N_{t_{mit},1}$	23.24	0.66
$\log L_{50\%}^P$	2.91	0.06	$\log N_{t_{mit},2}$	19.37	1.35
$\log F_{t_{mit}}^{TO}$	-5.93	1.18	$\log N_{t_{mit},3}$	20.04	0.69
$\log F_{7\&8.16}^{TO}$	-1.92	0.98	$\log N_{t_{mit},4}$	21.06	0.79

$\log F_{9\&10.16}^{TO}$	-1.85	0.94	$\log N_{t_{init},5}$	16.05	9.10
$\log F_{11\&12.16}^{TO}$	-1.80	0.89	$\log N_{t_{init},6}$	17.70	1.14
$\log F_{1\&2.17}^{TO}$	-1.82	0.88	$\log \pi_5$	-2.29	1.25
$\log F_{3\&4.17}^{TO}$	-5.13	0.98	$\log b_0$	0.35	0.15
$\log F_{5\&6.17}^{TO}$	-5.17	0.97	$\log \alpha$	-2.77	0.46
$\log F_{7\&8.17}^{TO}$	-1.98	0.76	$\log \beta$	0.99	0.05
$\log F_{9\&10.17}^{TO}$	-1.97	0.73			



3. Results

3.1. Assessment for the common squid

For the parameter estimation, some parameters were assumed to be known. I assigned input values to some parameters based on previous studies (Table 2.3): (1) μ_r and L_∞ (Sakurai et al., 2013); (2) β_0 and β_1 (Jo et al., 2019); (3) b_l (Lorenzen, 1996). The parameters in the length-fecundity relationship model, η_0 and η_1 , were assigned the point estimates obtained from the additional estimation with length-fecundity data (Fig. 2.1). Since there was no study on the sex ratio at age r (60 days old), a value of 0.5 was assigned to both male and female sex ratio over time: $\chi_{i,r}^{\sigma} = \chi_{i,r}^{\phi} = 0.5$. Thus, the model was able to estimate a total of 35 free parameters, including body growth parameters, fishing and natural mortality rate, population size, reproduction rate, gear selectivity parameters, and length-weight relationship parameters. The estimates of the free parameters and their standard errors are shown in Table 2.2.

The yield data for each fishery were not fitted well with the fitted values, but the fitted yield values followed the temporal trend of observed data for

each fishery (Fig. 2.2). The model fitted the length composition data for JIG and PS relatively poorly, but the modes of the fitted values moved along with the modes of the observed data over time (Fig. 2.3, Fig. 2.4). However, the model fit the length-weight data well (Fig. 2.5).

By considering the stock-recruitment relationship, model was able to present not only the 16 predicted values from May and June 2016 to November and December 2018, but also one projected value for recruitment and biomass in January and February 2019. The predicted recruitment was shown as seasonal trends in every year, with the highest recruitment in November and December and the lowest in March and April, and decreased compared to the predicted value one year ago (Fig. 2.6). In January and February 2019, recruitment was projected as 3.45×10^9 No. and declined compared to the previous time step.

The predicted biomass gradually decreased from May and June 2016 to November and December 2018, with fluctuations according to season (Fig. 2.7). The predicted biomass peaked at the summer season, July and August, and was lowest in winter, from January and February, each year. The highest and the lowest biomass was predicted as about 2.71×10^5 MT in July and August 2016, and 0.27×10^5 MT in November and December 2018. Biomass was projected as 0.17×10^5 MT in January and February 2019. A cohort was separated into males and females, using the sex ratio

at recruitment. It was also assumed that each sex undergoes different death processes by reproduction. Therefore, the biomass can be divided into the biomass of mature females and males. At all times, the mature biomasses were higher in females than males, and the biomasses in mature males were highest in July and August each year. The biomasses of mature females were highest in September and October every year. The biomasses of spawners who arrive at the spawning ground and lay eggs among the mature females were highest in September and October every year.

The size-specific natural mortality, $M(x)$, was predicted by estimating the parameters of equation (4). The predicted natural mortality was 5.88 bimonth^{-1} ($= 2.94 \text{ month}^{-1}$) at first length class 0.5cm, which rapidly declined in the higher length classes up to 0.18 bimonth^{-1} ($= 0.09 \text{ month}^{-1}$), to the last length class, 33.5cm (Fig. 2.8).

According to the fishing effort data, fishing mortality rates for JIG and PS were predicted by estimating the corresponding catchability, but fishing mortality rates for TO were estimated. The fully-selected fishing mortality rates for each fishery were represented as similar temporal fluctuations and different intensities (Fig. 2.9). The fishing mortality rate of JIG was predicted to be lowest at every March and April, but the fishing mortality rate of PS and TO were predicted to be lowest from

March and April to May and June every year. For each fishery, the fishing mortality rates in average (May and June 2016 – November and December 2018) were 0.07 bimonth⁻¹ for JIG, 0.003 bimonth⁻¹ for PS, and 0.15 bimonth⁻¹ for TO. These values accounted for 31%, 1%, and 68% of all the fishing mortality rates, respectively.

The predicted mean lengths for each age differed by cohort. These results originate from the different size-specific mortality over time. The average of the mean lengths of all cohorts from age 1 to 6+ were 1.49 cm, 5.09 cm, 10.68 cm, 16.68 cm, 21.71 cm, and 24.95 cm. The PMF of length distribution also differed by sex, and as the age increased, the mode of length distribution of females was larger than that of males at the same age (Fig. 2.10).

Table 2.3. Parameter values assigned to the length-based assessment model for the common squid, including growth (μ_r , L_∞), length-maturation (β_0 , β_1), natural mortality (b_1), length-fecundity (η_0 , η_1), and female ratio at recruitment ($\chi_{i,r}^\ddagger$) parameters. μ_r , L_∞ , β_0 , β_1 , and b_1 are taken from previous studies (Sakurai et al., 2013; Jo et al., 2019; Lorenzen, 1996). η_0 and η_1 are taken from the additional estimation with length-fecundity data.

Parameters	Input values
μ_r (cm)	1.47
L_∞ (cm)	33.7
β_0	11.537
β_1 (cm ⁻¹)	-0.615
b_1	0.305
η_0 (No. / cm ^{4.86})	$6.57 \cdot 10^{-3}$
η_1	4.86
$\chi_{i,r}^\ddagger$	0.5

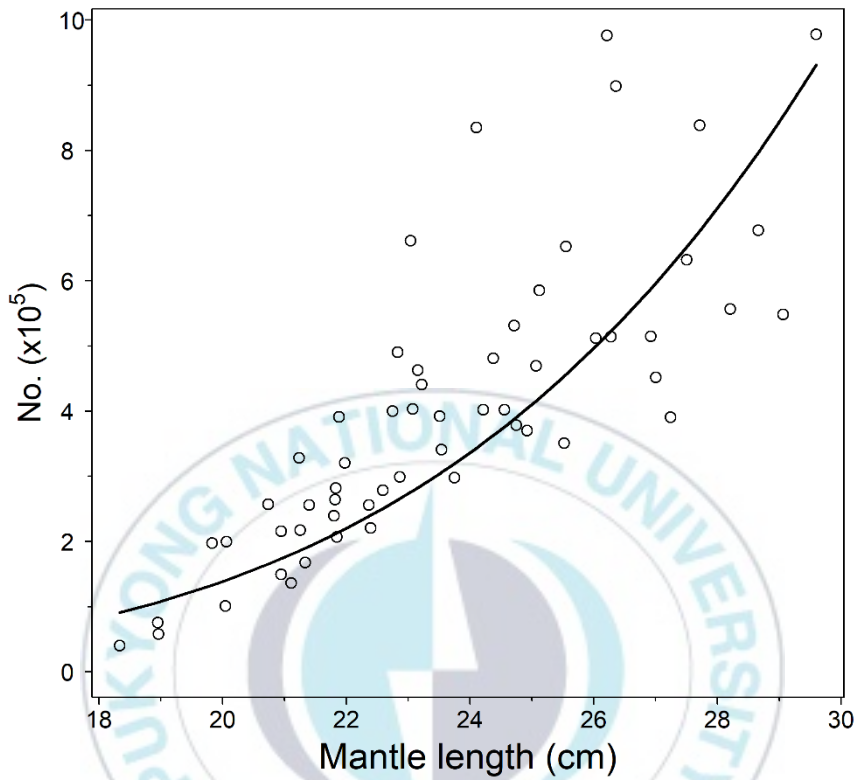


Fig. 2.1 Fitted fecundity at length $\hat{\phi}(x)$ from the length-fecundity data (Kim et al., 1997). The points denote data, and the solid line denotes the fitted line ($\phi(x) = \hat{\eta}_0 \cdot x^{\hat{\eta}_1} = 6.5 \cdot 10^{-3} \cdot x^{4.86}$). The vertical axis denotes the number of eggs ($\times 10^5$) and the horizontal axis denotes mantle length in cm.

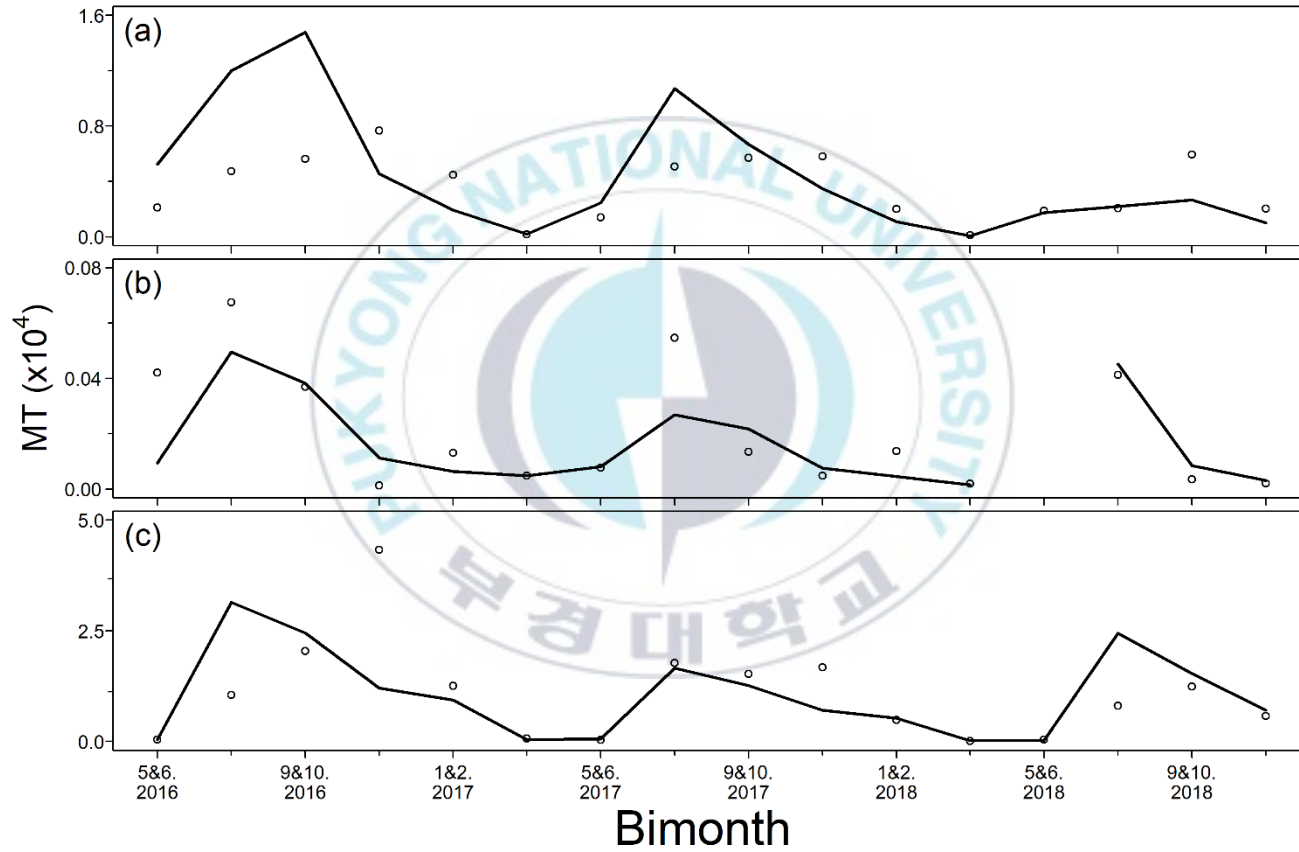
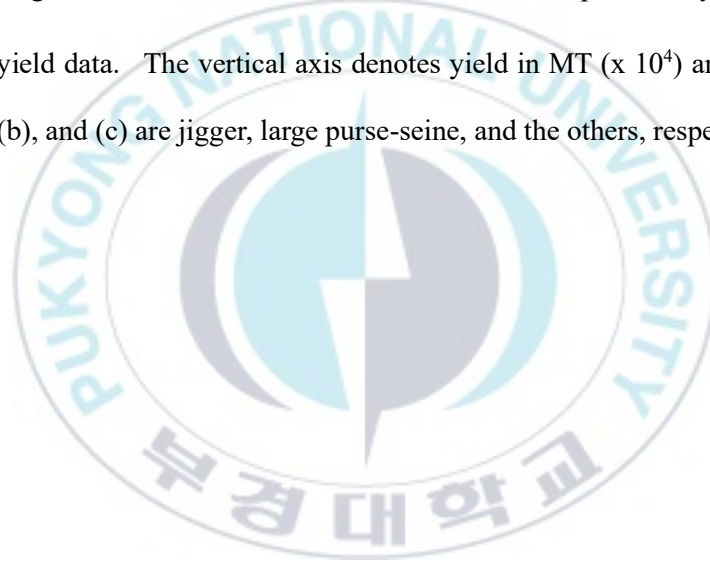


Fig. 2.2. Bimonthly yield data, Y_t^s , of the common squid from the three fisheries in Korea and the predicted yield for each fishery \hat{Y}_t^s from the length-based model. The solid line denotes the predicted yield from the model, and the points denote the observed yield data. The vertical axis denotes yield in MT ($\times 10^4$) and the horizontal axis denotes time (bimonth). Panel (a), (b), and (c) are jigger, large purse-seine, and the others, respectively.



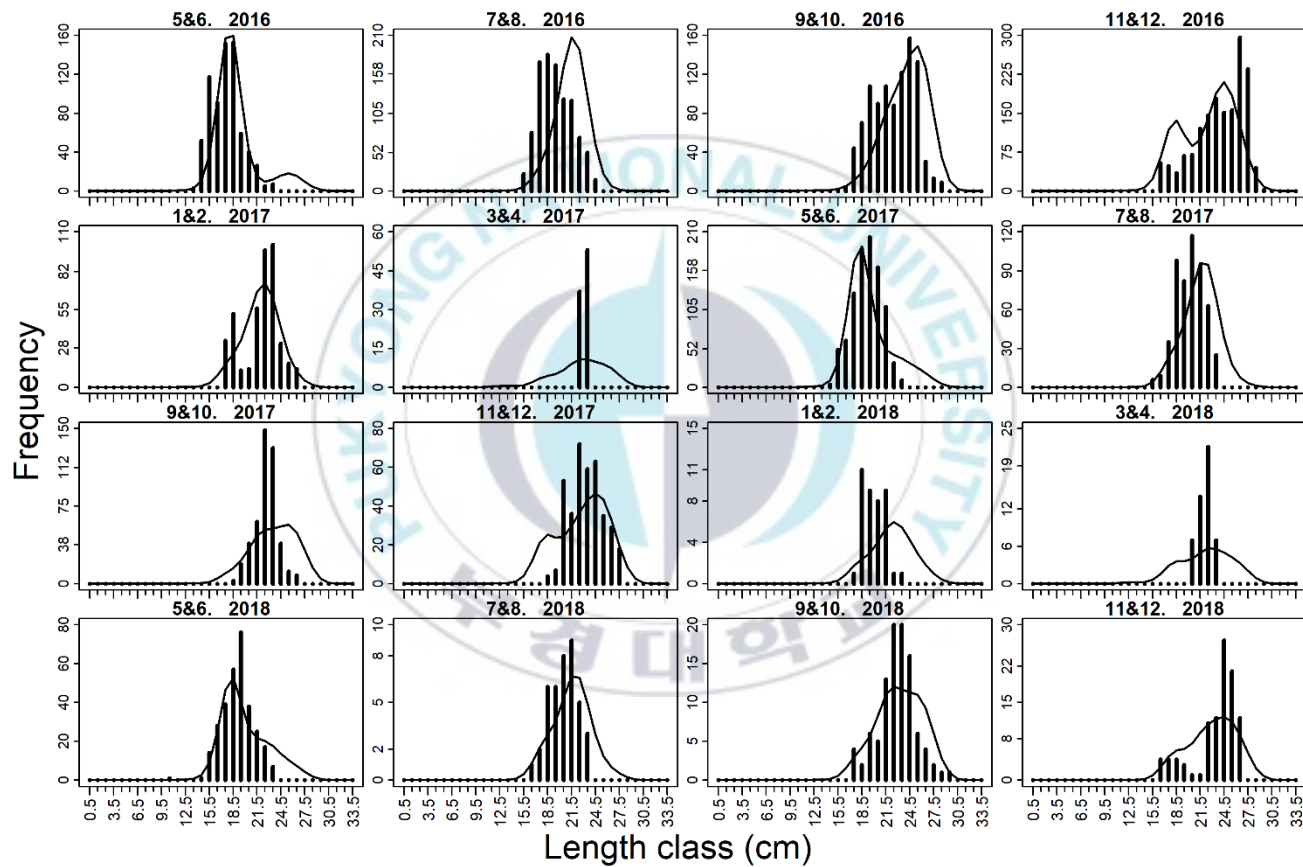
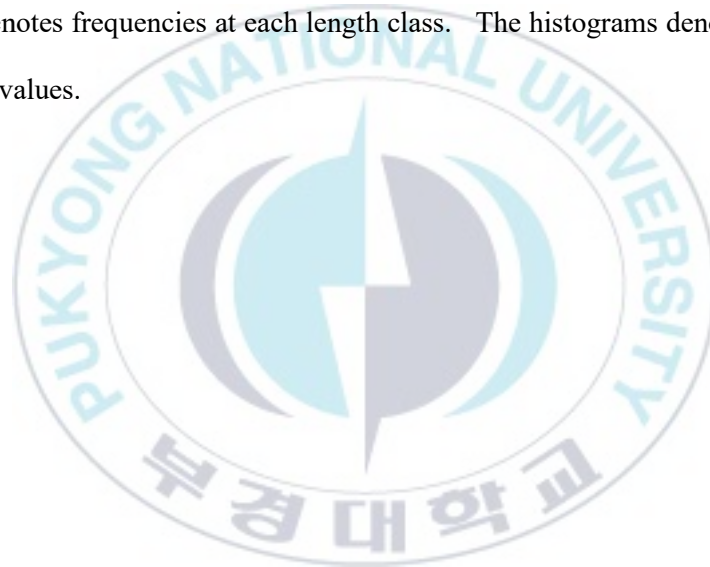


Fig. 2.3. Predicted length frequency of jigger fishery from length-based model and observed length composition data from May and June 2016 to November and December 2018. The horizontal axis denotes length classes with width of 1cm and the vertical axis denotes frequencies at each length class. The histograms denote the observed data, and the solid lines denote predicted values.



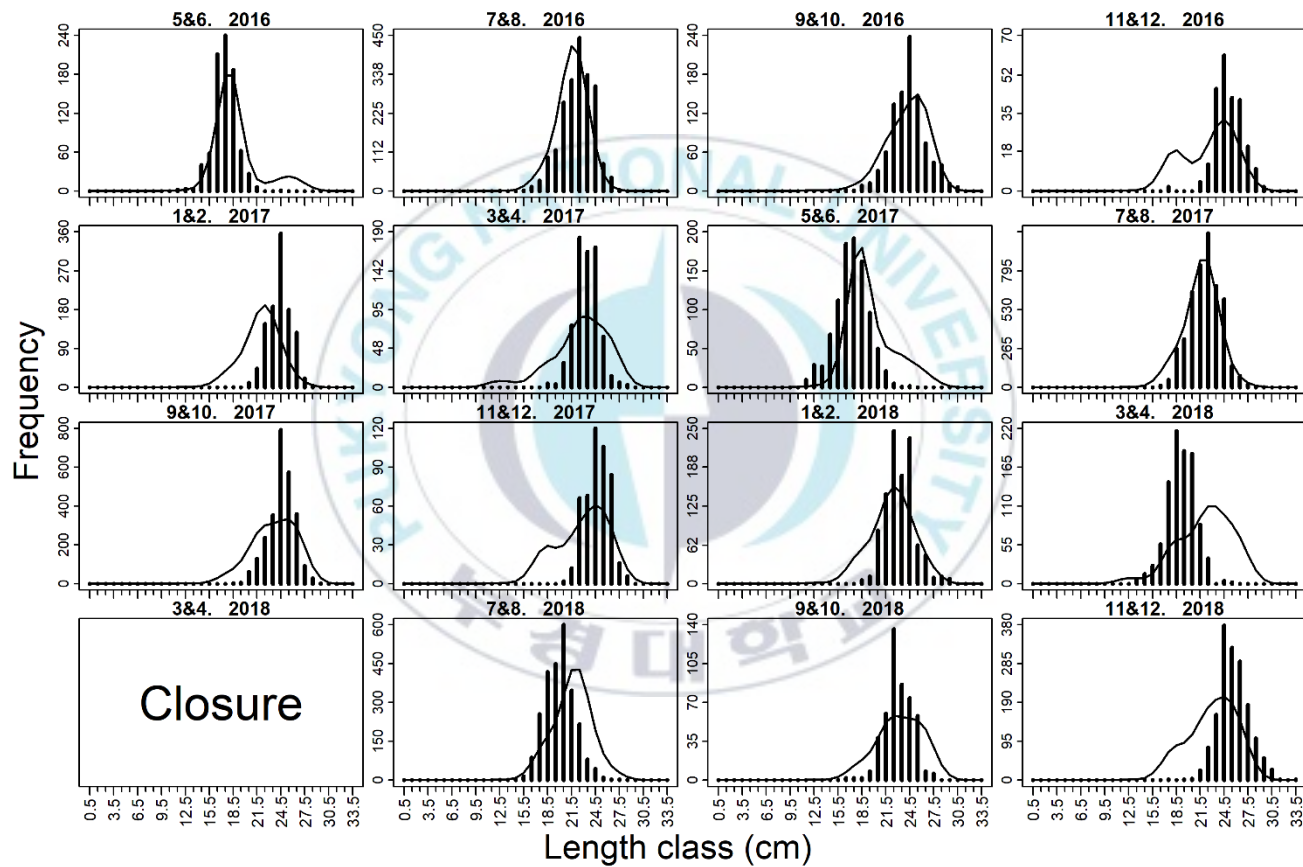
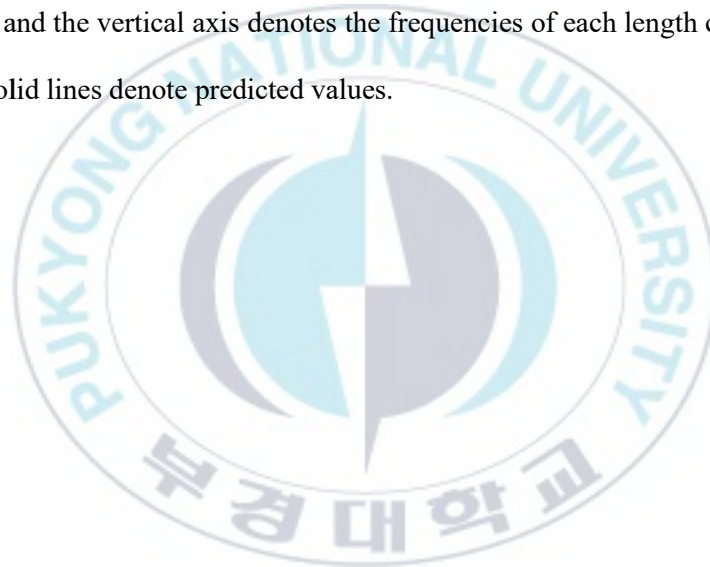


Fig. 2.4. Predicted length frequency of large purse-seine fishery from length-based model and observed length composition data from May and June 2016 to November and December 2018. The horizontal axis denotes length classes with a width of 1cm and the vertical axis denotes the frequencies of each length class. The histograms denote the observed data, and the solid lines denote predicted values.



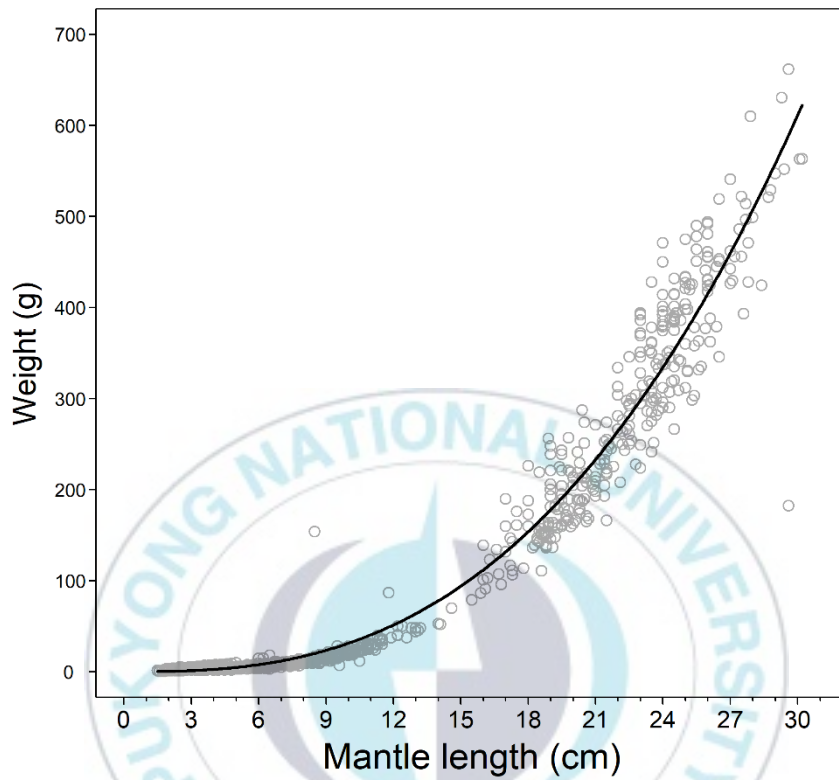


Fig. 2.5. Predicted weight at length $W(x)$ from the length-based model. Gray points denote observed data (1,091 squid), and the solid line denotes the predicted value ($W(x) = \hat{\alpha} \cdot x^{\hat{\beta}} = 0.06 \cdot x^{2.7}$). The horizontal axis denotes mantle length in cm, and the vertical axis denotes body weight in grams.

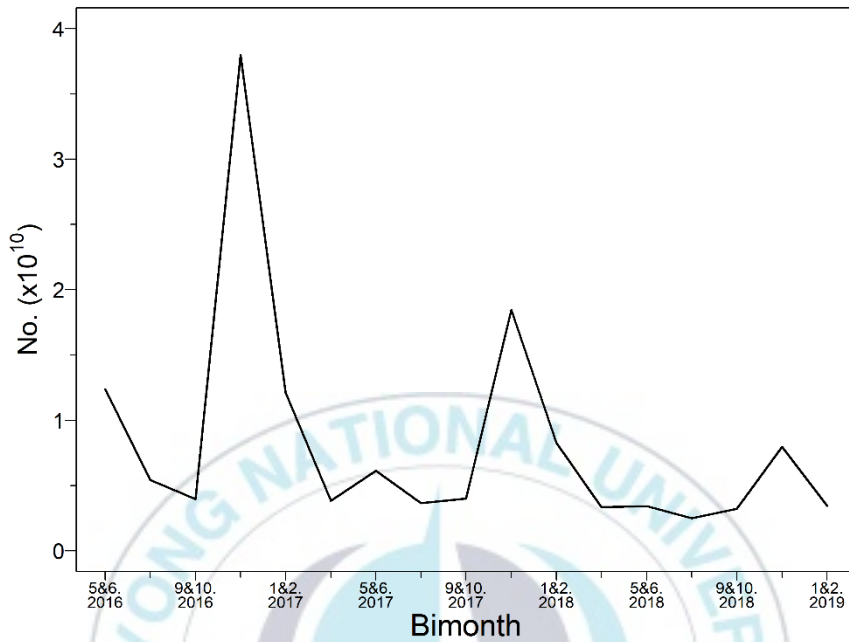


Fig. 2.6. Predicted bimonthly recruitment from May and June 2016 to November and December 2018, and projected recruitment in January and February 2019 of the common squid stock. The vertical axis denotes recruitment in number ($\times 10^{10}$) and the horizontal axis denotes time (bimonth).

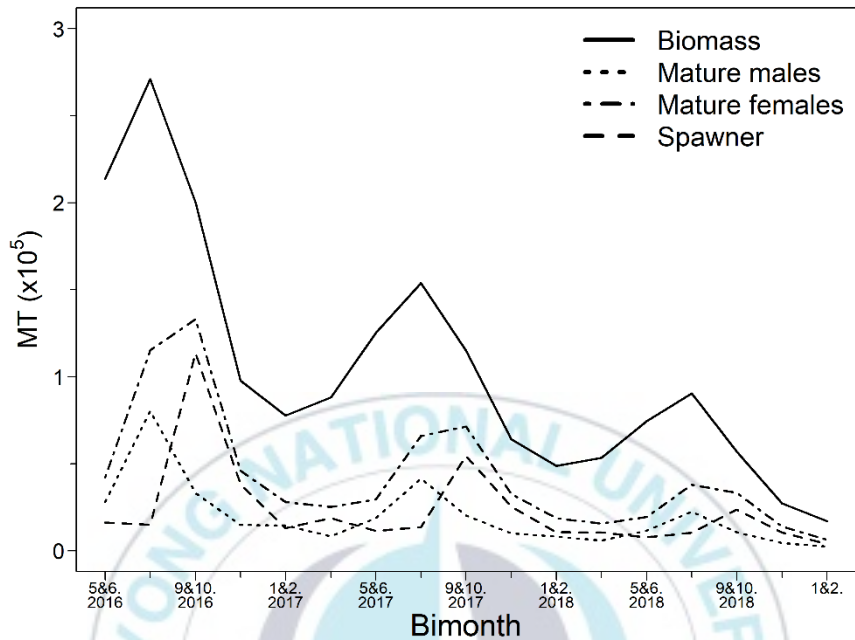


Fig. 2.7. Predicted bimonthly biomass from May and June 2016 to November and December 2018 and projected biomass in January and February 2019 of the common squid stock. Solid line denotes the predicted biomass of the common squid stock, the dotted line denotes the predicted biomass of mature males, dash-dotted line denotes the predicted biomass of mature females, and dashed line denotes the predicted biomass of spawners. The vertical axis denotes biomass in MT ($\times 10^5$) and the horizontal axis denotes time (bimonth).

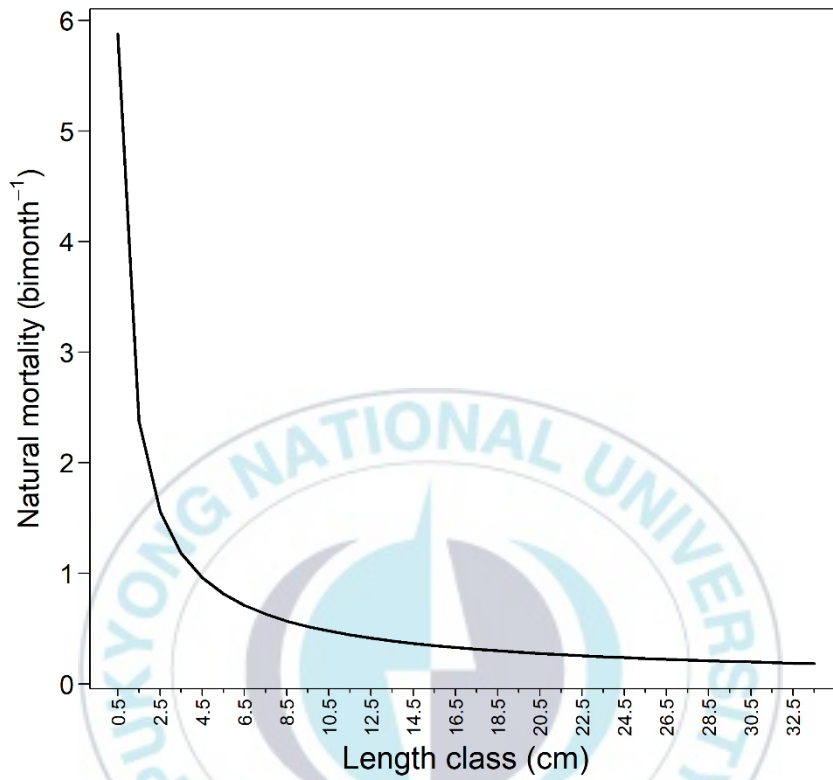


Fig. 2.8. Predicted size-specific natural mortality rate $M(x)$. The vertical axis denotes instantaneous natural mortality rate (bimonth⁻¹) and the horizontal axis denotes length class in cm.

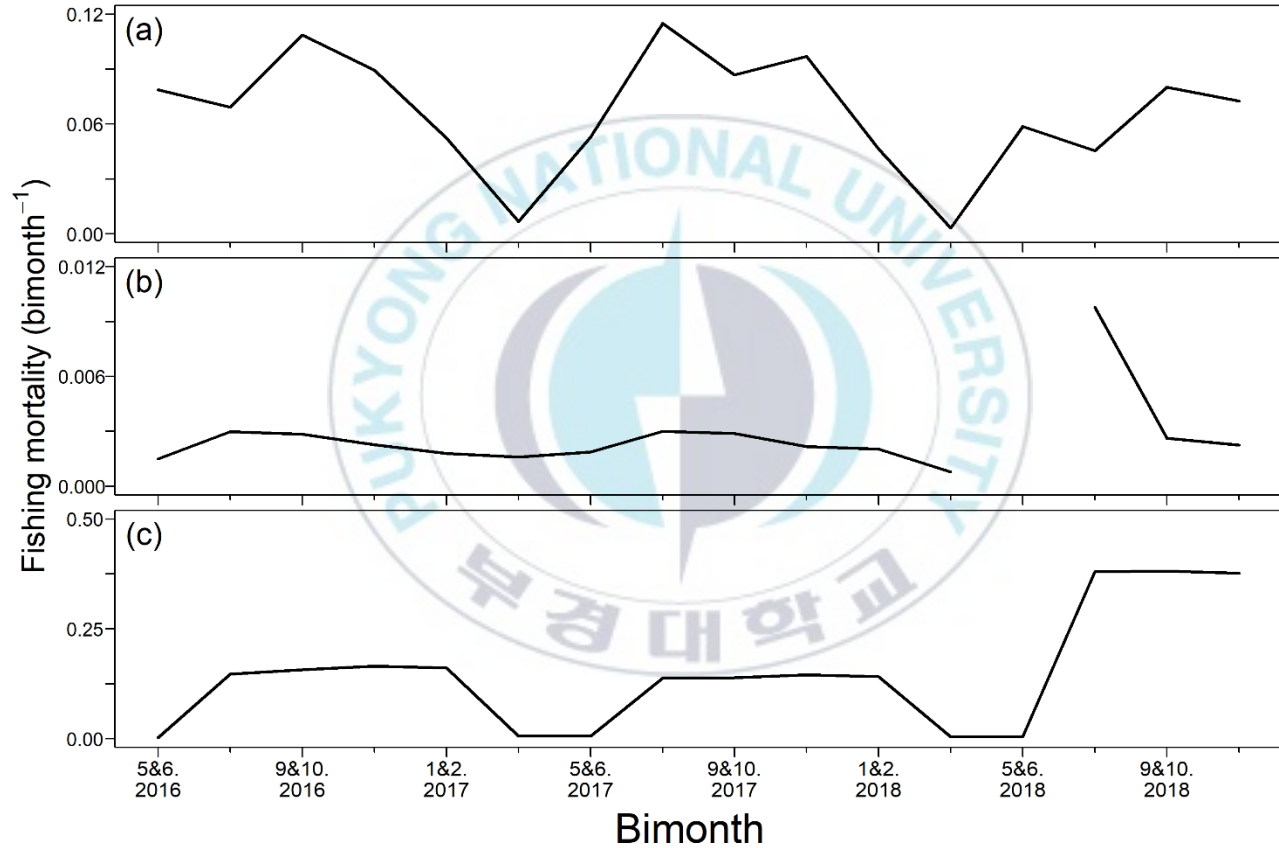


Fig. 2.9. Predicted bimonthly instantaneous fishing mortality rates of (a) jigger, (b) large purse-seine, and (c) the other fisheries. The vertical axis denotes instantaneous fishing mortality (bimonth^{-1}) and the horizontal axis denotes time (bimonth).



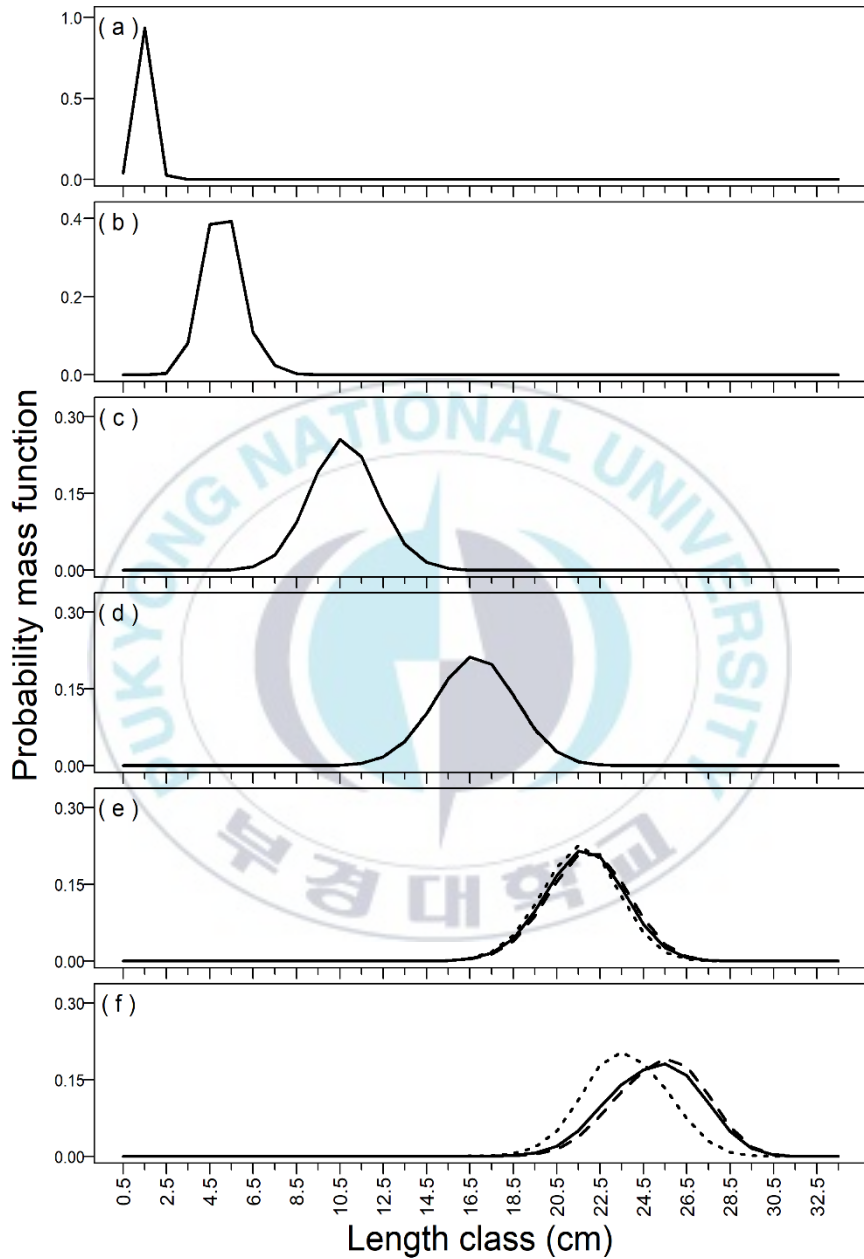
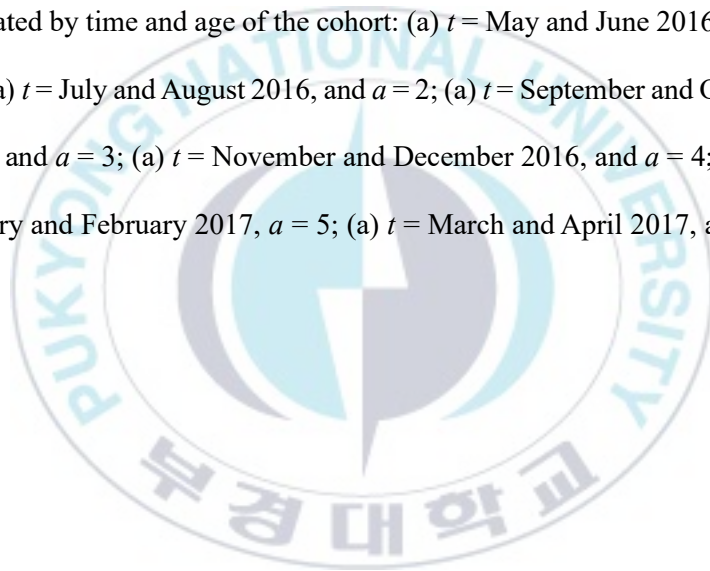


Fig. 2.10. Predicted probability mass functions (PMF) of length distribution by age of the cohort recruited in May and June 2016. Solid lines denote the predicted PMF of a cohort ($f_{t,a}(x)$), dotted line denotes the predicted PMF of a cohort of males ($f_{t,a}^{\delta}(x)$), and the dashed line denotes the predicted PMF of a cohort of females ($f_{t,a}^{\phi}(x)$). Panels are separated by time and age of the cohort: (a) $t =$ May and June 2016, and $a = 1$; (a) $t =$ July and August 2016, and $a = 2$; (a) $t =$ September and October 2016, and $a = 3$; (a) $t =$ November and December 2016, and $a = 4$; (a) $t =$ January and February 2017, $a = 5$; (a) $t =$ March and April 2017, and $a = 6+$.



3.2. Model performance

I evaluated the performance of the length-based model for the common squid with respect to the number of convergences, the goodness-of-fit, and the relative differences of free parameters under different ME scenarios.

To count the convergences of 1,000 iterations for each ME scenario, I set the criteria for convergence as follows: (1) indication for convergence using the 'nlsmin' function in the R software; and (2) maximum gradient < 0.001 . In 1,000 iterations of three levels of ME scenarios, with log normal errors of CV of 10%, 30%, and 50%, convergences were 914, 740, and 570, respectively. Thus, convergence decreased as the level of measurement errors increased. The larger the level of measurement errors, the greater the uncertainty in simulated data sets, so this result seemed to be acceptable.

To compare the goodness-of-fit for each scenario, I used the residual sum of squares (RSS) for each random vector, \mathbf{m}^J , \mathbf{m}^P , \mathbf{Y}^J , \mathbf{Y}^P , \mathbf{Y}^{TO} , and \mathbf{W} , which belongs to the likelihood components (Table 2.4). Residuals were calculated by subtracting the simulated data from the fitted values obtained from model estimation using simulated data. The RSSs of each random vector in all ME scenarios were less than the RSSs from actual data sets, except for weight at length, \mathbf{W} . RSS for \mathbf{W} was invariant

among all scenarios, and almost equal to a result from actual data sets. The RSS for two multinomial variables (\mathbf{m}^J , \mathbf{m}^P) and three lognormal variables (\mathbf{Y}^J , \mathbf{Y}^P , \mathbf{Y}^{TO}) gradually increased as the MEs in yields of each fishery increased.

My model includes various parameters to reflect the biological characteristics of the common squid. Uncertain parameters, such as the variance of length distribution of a recruitment, a parameter in the natural mortality rate, and the spawning migratory rate were estimated. Thus, I used the *RD* statistic to evaluate the estimability of parameters in my model. The *RD* was calculated based on the maximum likelihood estimates of each parameter for the converged case of each scenario. Because uncertainties in the process of fishing mortality of TO were incorporated into each simulated data set, the true values of time-series fishing mortality for TO varied in each iteration, except for $F_{t_{init}}^{TO}$, which is estimated as a free parameter regardless of penalized likelihood. Thus, I evaluated the distribution of the *RD* for 20 free parameters, excluding 15 fishing mortality rates of TO from July and August 2016 to November and December 2018. The distributions of *RDs* for the converged case of the scenario were displayed using box plots, and the different levels of ME in yields for each fishery were compared (Fig. 2.11). For each scenario, the

distributions of RD s were shown to be quite precise overall, but the estimates of $\log F_{t_{mit}}^{TO}$ and $\log \pi_5$ were not precise compared to the other parameters. The distributions of RD were more dispersed, with negative bias occurring in the higher levels of ME. The RD s of estimates for parameters involved in body growth ($\log \sigma_r^2$, $\log G$, and $\log \sigma_G$), size-specific gear selectivity (γ^J , γ^P , $\log L_{50\%}^J$, $\log L_{50\%}^P$), and length-weight relationship ($\log \alpha$, $\log \beta$) were quite robust, even at high levels of ME. The RD s of estimates for parameters involved in mortality ($\log q^J$, $\log q^P$, $\log F_{t_{mit}}^{TO}$, $\log b_0$) and reproduction ($\log \pi_5$) were very sensitive to the level of ME.

Table 2.4. Mean value of residual sum of squares (RSS) of six variables constituting the likelihood function under different levels of measurement error scenarios from 1,000 replicates. In the scenarios, $CV_{10\%}$, $CV_{30\%}$, and $CV_{50\%}$ indicate the measurement error in all data sets with 10%, 30%, and 50% levels of coefficient of variation. Scenario ‘Actual data’ refers to the actual data sets, and is shown for comparison with the simulation experiments.

Scenarios	\mathbf{m}^J	\mathbf{m}^P	$\log \mathbf{Y}^J$	$\log \mathbf{Y}^P$	$\log \mathbf{Y}^{TO}$	\mathbf{W}
Actual data	261095.4	1424365.7	6.7	10.7	5.8	784160.6
$CV_{10\%}$	14239.6	13314.7	0.1	0.1	0.4	786188.7
$CV_{30\%}$	15926.5	14822.2	1.2	1.0	1.5	786221.0
$CV_{50\%}$	18463.5	17444.0	3.1	2.6	3.4	786276.4

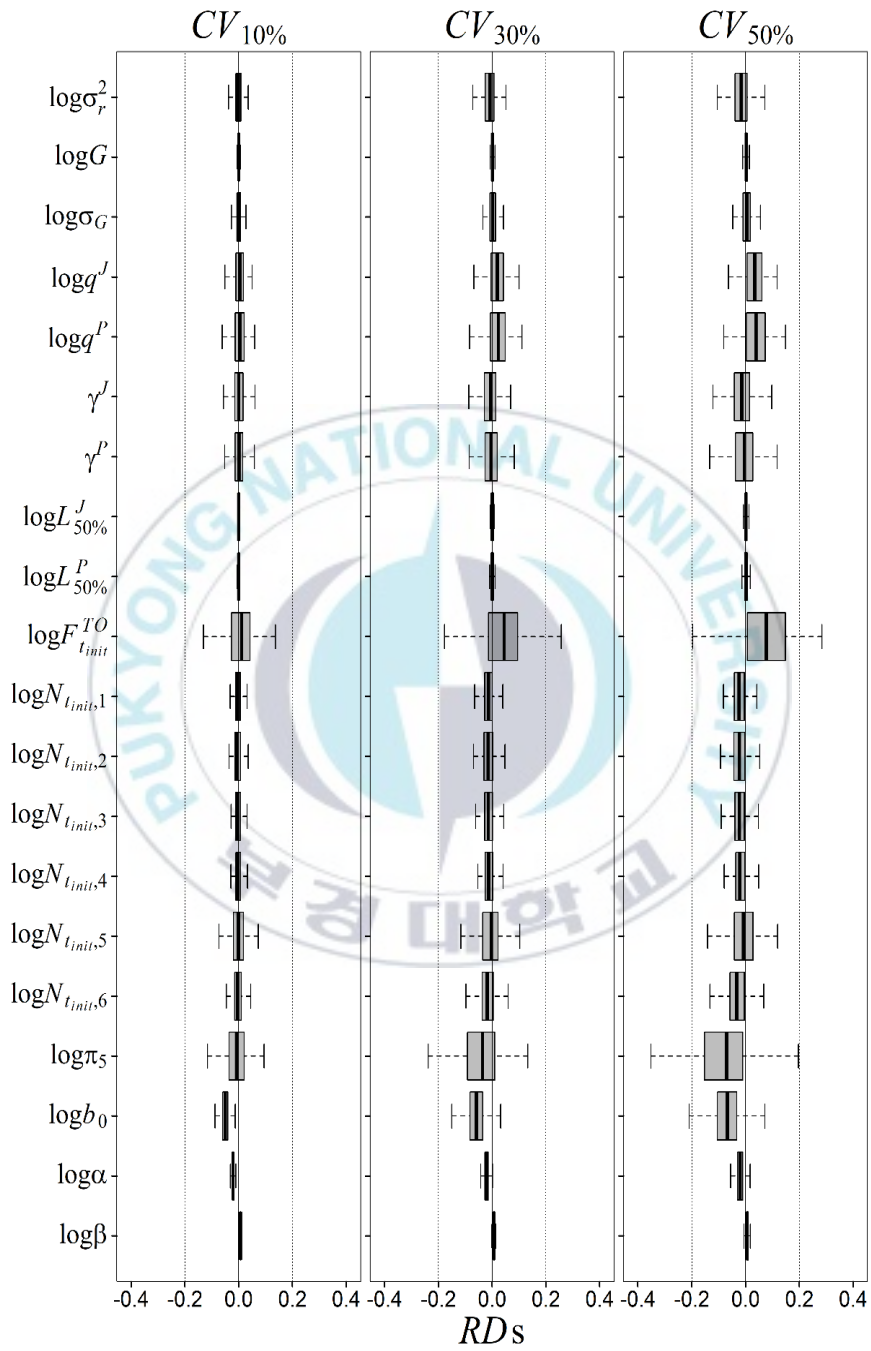


Fig. 2.11. Box plots of relative differences (*RDs*) of estimates for each level of measurement error. Scenarios $CV_{10\%}$, $CV_{30\%}$, and $CV_{50\%}$, are the measurement errors in all yield data sets with 10%, 30%, and 50% levels of coefficient of variation. Boxes represent the interquartile range (25th – 75th percentile). Bold lines in the boxes indicate the median value of *RDs*, and lines outside the whiskers indicate the upper and lower fences.



4. Discussion

Cephalopods exist in all marine habitats worldwide, and make up a large part of the total global biomass of all marine species. These organisms are important biologically, commercially, and scientifically (Fries, 2011). However, assessing the stock of cephalopods is an ongoing challenge, due to a lack of information about their migration, reproduction, body growth, and mortality, and their environmental sensitivity. The common squid is one such species. Under these circumstances, I developed an assessment model for the common squid, using length composition data. My model is based upon Quinn's length-based model, but includes the situation of multiple fisheries in Korean waters and biological properties of the common squid, resulting in outcomes that precursor model did not address.

Parameter estimation was performed by minimizing the objective function value as the negative log-likelihood function, which found the best fit between a model and data. In actual data example, the yield data and the length composition data for each fishery were not fitted well with the model values. The model is designed to catch the squid for each fishery from a single population at the same time. These results were considered that the model integrates the information from each fishery

data set. In simulation studies, goodness of fit in the model for each data set were deteriorated as the ME increased. Because I assumed that random vectors in the objective function are independent, It is therefore problematic that the goodness of fit for two multinomial variables (\mathbf{m}^J , \mathbf{m}^P) are affected by the measurement errors only for the yields of each fishery. It is thought that this result originates from fishing mortality rate related with yield. Because fishing mortality is product of size-specific gear selectivity and time-specific fishing intensity, even the fish with low selectivity will eventually be caught at high level of fishing intensity. The predicted catch composition will also differ from that obtained under different level of fishing intensity. Thus, predicted catch composition obtained from Baranov catch equation depends highly on fishing intensity (Branch, 2009), which means that there is an interaction between the yield (lognormal variable) and catch composition (multinomial variable).

I used the Gompertz growth model to account for the body growth of the common squid, and my model was able to estimate the parameters related to body growth: σ_r^2 , G , and σ_G . The estimation of these parameters was very precise and unbiased. Therefore, the Gompertz growth model seems to be appropriate for explaining the body growth of the common squid, whose instantaneous growth rate changes as age

increases. This length-based model can be applied to other fish species with differences in body growth rate between the larval and adult stages.

Quinn et al. (1998) assumed that the first eight recruitments in the series are forced to have the same trend as the following year, so they used these eight recruits as derived parameters, but the other recruitments were set as free parameters. However, I derived the recruitment parameters by using spawner-recruitment model. The relationship between the parental fish and the resulting recruitment has been described in many studies as Beverton and Holt (1957) and Ricker (1954) model. Beverton and Holt model assumed that recruitment approached toward asymptotic value at high spawning stock biomass. Ricker model assumed that the peak level of recruitment occurred at an intermediate spawning stock biomass. I also tried to estimate the free parameters using these two stock-recruitment models, but failed to estimate the parameters. As an alternative, recruitments were linked to spawners at the previous time-step, using a length-fecundity relationship (Kim et al., 1997). With this extension, my model was able to reduce the number of free parameters, and project the abundance of this stock in January and February 2019. Given that I defined recruits as being 60 days old, predicted recruitment involved individuals born two months previously. I separated recruitment by birth date and identified three cohorts according to different peak spawning

seasons: winter, from January to April; summer, from May to August; and autumn, from September to December (Kim et al., 2011; Kim and Kang, 1995). The autumn cohort was predicted to be the largest, winter was second, and summer was the smallest. However, there was no evident gap between the winter and summer cohorts. This result conflicts with previous research into common squid (Sakurai et al., 2013). Sakurai (2013) stated that the autumn and winter cohorts are the largest. This may be due to the migration route of the winter cohort. The winter cohort is born in the East China Sea off Kyushu Island, south of Japan, then some of squid migrate to feed in the northern East Sea of Korea, where they might be caught by Korea fisheries, while the majority migrate in the waters off eastern Japan (Sakurai et al., 2013; Kidokoro et al., 2010).

Because the natural mortality rate is confounded by other parameters, the estimation of the natural mortality rate is difficult (Fu et al., 2000). Thus, the natural mortality rate is assumed to be known, or to be a non-time varying constant in many models. In my model, the natural mortality rate was modelled as a power function of the body length, and can be estimated as a parameter, b_0 , in the natural mortality function. In terms of RD , the estimation of b_0 is relatively precise, but is negatively biased. This result originates from the estimation of parameter α , which determines the magnitude of the natural mortality rate, along with

b_0 . Because the estimation of the two parameters α and β in the length-weight relationship was independently supported by length-weight data, these estimates were too precise and robust to make b_0 biased. Millar and Hyun (2018) compared two approaches to natural mortality rate in the age-structured model as Lorenzen (1996) equation (= allometric relationship of natural mortality to body weight) and constant, which also showed worse performance in the case of Lorenzen equation.

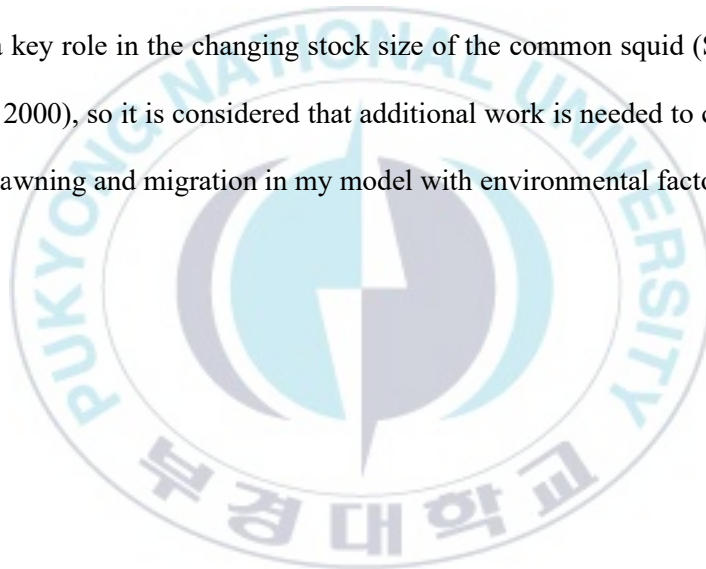
About 25 fisheries in Korea exploit the common squid, and the yield in each fishery is obtained from 'one common squid population'. It is therefore necessary to consider yields in all fisheries to assess the population. However, there are problem in parameter estimation, and data are not available for all 25 fisheries. Thus, I separated all fisheries into three fleets, depending on the availability of length composition data. Due to the lack of length composition data, the fishing mortality rate for TO, unlike JIG and PS, is not specified for the length class. So, it is reasonable to use the concept of pulled mean for lengths. The fishing mortality rate of JIG was predicted to be lowest at every March and April, but the fishing mortality rate of PS and TO were predicted to be lowest from March and April to May and June every year. Considering that the seasonal closure of the JIG is in April each year, and the seasonal closure of the other fisheries is from April to May each year in Korea, these results

were reasonable. The fishing mortality rates for each fishery were predicted as being high from July to the winter season each year, which is consistent with the total allowable catch (TAC) for the common squid is allocated in July every year. In the results of the simulation experiments, the estimation of $F_{t_{init}}^{TO}$ was shown to be more biased than q^J and q^P , which determine the corresponding fishing mortality rate, at high levels of ME. As the ME of the yield increased, the variability of the simulated yield increased, and the variability of the total fishing mortality rate also increased. Here, the fishing mortality rates for JIG and PS, which constitute the total mortality rate, are relatively robust when estimated using fishing effort data, whereas the fishing mortality for TO is impacted by the variability of the total fishing mortality rate. The estimation of $F_{t_{init}}^{TO}$ also appeared to be less precise than that of other parameters, because uncertainties in the fishing mortality of TO was incorporated into each iteration. For each fishery, the estimation of parameters related to the fishing mortality rate (q^J , q^P , $F_{t_{init}}^{TO}$) were positively biased, which means that the fishing mortality rates of all fisheries were highly estimated. On the other hand, parameters (b_0 , α) that determines the magnitude of natural mortality rate were negatively biased, which means that the natural mortality rate was estimated to be low. Consequently, the model appears

to be trying to keep the total mortality rate invariant as the ME of the yield increases.

Quinn et al. (1998) were able to estimate the growth parameter, gear selectivity, and fishing mortality of each sex by classifying the dynamics of each sex using length composition data for each sex. However, I separated the cohorts into male and female in the absence of length composition data for each sex. There were two reasons for separating a cohort into males and females: (1) the common squid, as well as cephalopods, has distinctly different rates of death by reproduction between males and females; (2) spawner, females capable of laying eggs, must be defined as part of a recruitment. Therefore, I was not able to distinguish between males and females in terms of body growth and fishing mortality, unlike Quinn et al. (1998), but I was able to discriminate the dynamics of each sex without any data on sex, using spawner-recruitment relationship and mortality by reproduction. However, the estimability of the arrival rate at spawning ground at age 5, π_5 , appears to be problematic, as a result of model evaluation. This problem also relates to the estimation of the abundance of age 5 at time t_{init} , $\log N_{t_{init},5}$. The estimation of the abundance of each age at time t_{init} , $\log N_{t_{init},1}$ - $\log N_{t_{init},6+}$, were negatively biased at high levels of ME, but estimation

of $\log N_{t_{mir},5}$ was not biased and precise than that of the others. Kidokoro et al. (2010) showed that the spawning migration routes and the spawning ground changed after the regime shift in the late 1980s, based on tagging experiment. It is thought that the spawning ground and the spawning migration routes of the common squid are closely connected with environmental changes. Such changes in spawning are thought to play a key role in the changing stock size of the common squid (Sakurai et al., 2000), so it is considered that additional work is needed to connect the spawning and migration in my model with environmental factors.



II. How should we randomly sample marine fish landed at Korean ports to estimate the length frequency distribution of those fish?

1. Introduction

Fishery stock resources are being used and developed in various fields of human activities. To facilitate continual conservation and use, the status of the resources must be understood through fishery stock assessment, and appropriate management must be carried out. Fishery stock assessment can be performed using different models, depending on the available data. The data are generally samples collected when it is impossible to examine the entire population, and should reflect the characteristics of the population. Age-structured models, which are currently the preferred method for fishery stock assessment, require long-term accumulated age data, which is difficult to collect because of time and cost. An alternative method is a length-based model using body length composition data. The length-based model can detect variations in population size by modelling the virtual age structure of the population, classifying the cohorts, detecting temporal changes in body length for each

individual, and tracking the growth and death of the cohorts. Therefore, length composition data, which is easier to collect than age data, is important.

In Korea, length composition data was collected after going through the ‘arrangement process’ (BCFM, 2020; Fig. 3.1). The fish sampled were collected from fresh and frozen fish, excluding live fish. Frozen fish were sorted by species and body size by the crew, and then the fish sorted are placed into a box by a certain weight before entering the port. Fresh fish are landed in a randomly mixed state by species and body size, and the sorting and filling processes are carried out at the port. The whole process of sorting and filling is called an ‘arrangement process’. After the arrangement process, all fish landed are contained in boxes by body size group and are then sampled.

The current sampling method is to collect the samples from fish sorted by body size groups (e.g., very small, small, medium, large, very large) in proportion to the number of boxes in body size groups (Seong-woo Goo, Korea Fisheries Resources Agency, Busan, Republic of Korea, personal communication; NFRDI and PKNU, 2004). This is a sampling method using prior information about the number of boxes in body size groups of the population of fish landed; a stratified random sampling method.

Stratified random sampling is a method of separating a population into

several strata according to specific criteria, and collecting samples from each stratum. The strata should be collectively exhaustive and mutually exclusive. Even if the number of samples to be collected is small, stratified random sampling has the advantage of collecting samples representing the population (Lohr, 1998; Scheaffer et al., 1971). According to the definition of the stratified random sampling, fish landed are sorted into several body size groups with homogeneous body size. Thus, it is necessary to collect samples by body size groups proportional to the number of fish sorted by body size groups.

In this chapter, I performed simulation experiments to evaluate whether or not the length composition data sampled using the current sampling method can represent the length composition of the fish landed, and suggested that an alternative sampling method using the sampling weights as the number of fish sorted by body size group should be applied.

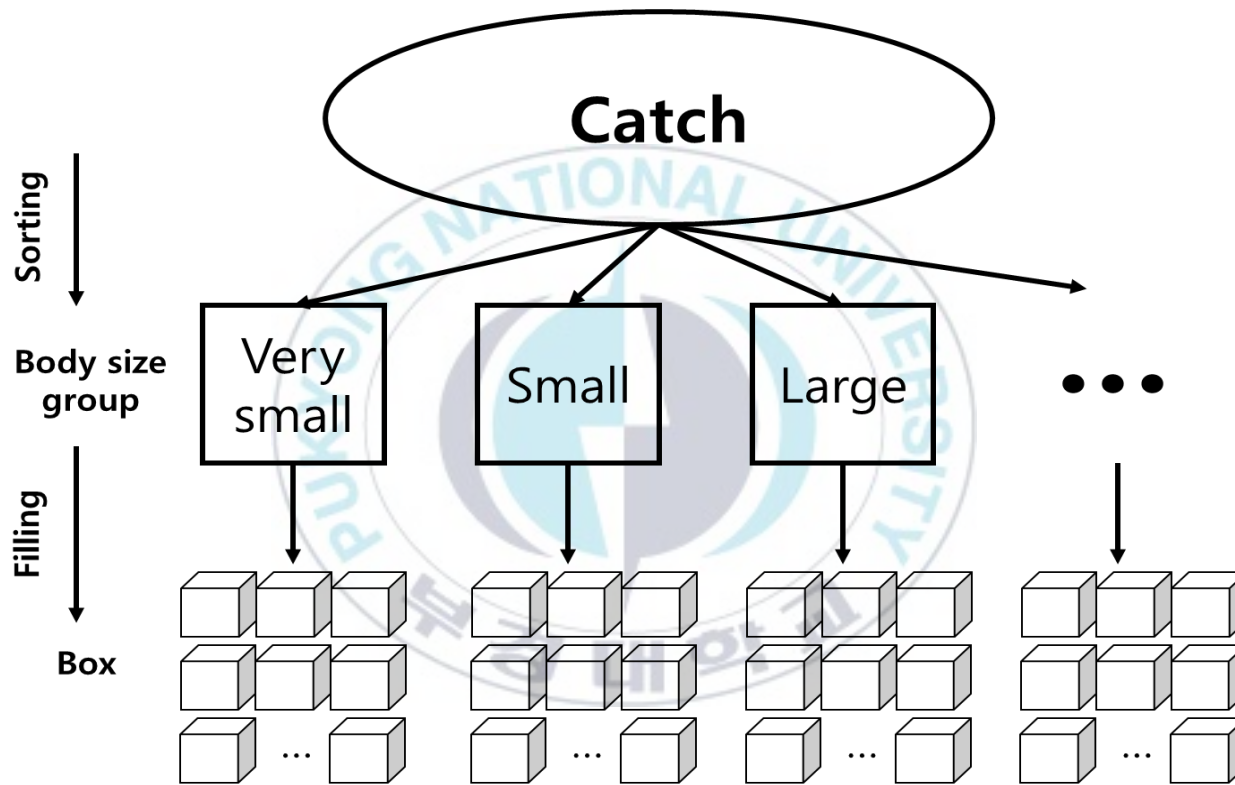


Fig. 3.1. Process of arranging fish landed.

2. Methods

2.1. Simulated length composition data

All symbols used in this chapter are summarized in Table 3.1. To generate the simulated length composition data, the data sampling process was separated into landing, arrangement, and data collection, in time order.

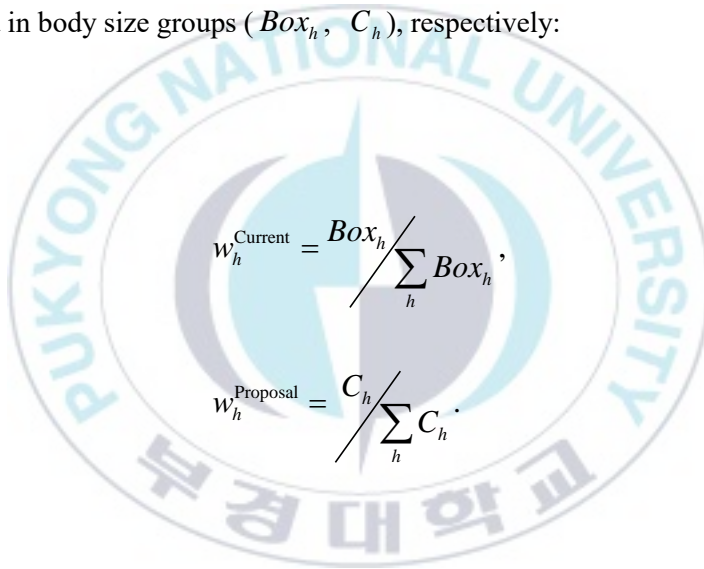
At landing time, all individuals landed (i) have their own body length (X_i) and body weight (W_i). The body weight of each fish landed was generated by the lognormal error of an allometric length-weight relationship,

$$W_i = \alpha \cdot (X_i)^\beta \cdot \exp[\varepsilon_i]; \quad \varepsilon_i \sim N(0, \sigma_w^2).$$

At the arrangement time, the fish landed goes through the sorting process, classifying the fish into several body size groups according to the body length section of each group, where length sections do not overlap between groups. When the sorting process is completed, the number of fish sorted in body size group h (C_h) is obtained, and the filling process is carried out. In the filling process, each box is filled with fish according

to a certain weight, W^{Box} , which is set differently for each fish species. When the filling process is complete, the number of boxes in body size group h (Box_h) can be obtained.

The sampling weights for the ‘current’ and ‘proposal’ sampling method ($w_h^{Current}$, $w_h^{Proposal}$) are proportional to the number of boxes and fish sorted in body size groups (Box_h , C_h), respectively:



$$w_h^{Current} = \frac{Box_h}{\sum_h Box_h},$$

$$w_h^{Proposal} = \frac{C_h}{\sum_h C_h}.$$

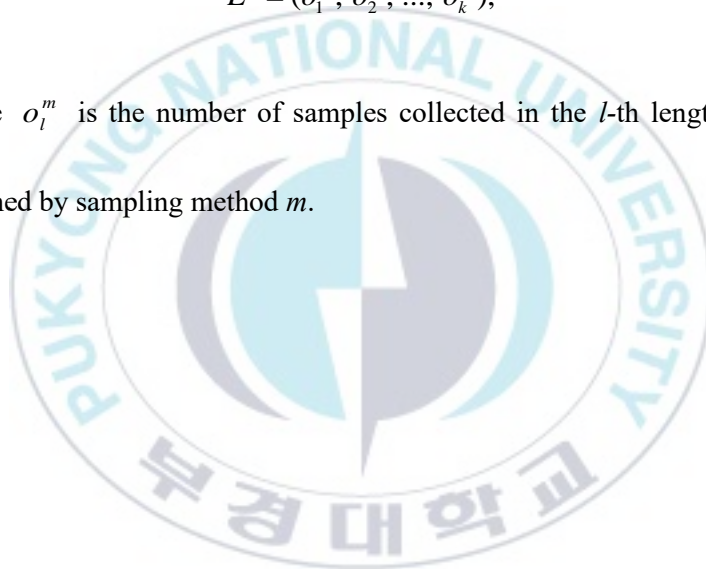
For each sampling method (m), the sample size taken from body size group h (S_h^m) is obtained by multiplying total sample size (S) and corresponding sampling weight:

$$S_h^m = S \cdot w_h^m; \quad m = \{\text{Current; Proposal}\}.$$

The simulated length data are collected from each body size group by corresponding sample size (S_h^m), and discretized into k length classes, resulting in simulated length composition data (L^m):

$$L^m = (o_1^m, o_2^m, \dots, o_k^m),$$

where o_l^m is the number of samples collected in the l -th length class obtained by sampling method m .



2.2. Inference of parameters

For each sampling method, simulated data was used to estimate the k length composition rates of fish landed, by assuming that length composition data followed a multinomial distribution:

$$L^m \sim \text{multinomial}(S, \boldsymbol{\pi})$$

$$\boldsymbol{\pi} = (\pi_1, \pi_2, \dots, \pi_k)$$

where $\boldsymbol{\pi}$ is k length composition rates. Thus, I constructed an objective function (Obj^m) as the negative log-likelihood function of a multinomial distribution (ℓ):

$$Obj^m = -\ell(\boldsymbol{\pi} | L^m).$$

The point estimates of k length composition rates and their uncertainty were estimated by numerical optimization using the TMB package in R. Using TMB, it was possible to calculate the standard error of the estimate for the last length composition rate, π_k , which is difficult to calculate using an analytical method.

Table 3.1. List of symbols. Values used in the simulation are under “Setting values”.

Symbols	Definition	Setting values
i	Index for individual	
C	Number of fish landed.	0.1 and 1 million
X	Lengths (cm) of all fish landed.	
W	weights (gram) of all fish landed.	
α, β	Parameters in the allometric length (in cm)-weight (in gram) relationship.	$\alpha = 0.003,$ $\beta = 3.425$
σ_w^2	Variance of error term in allometric relationship.	0.01 g ²
h	One of the five size groups.	

C_h	Number of fish landed which belong to size group h .	
W^{Box}	Body weight of fish landed in a box.	18 kg
Box_h	Number of boxes, which belong to size group h .	
m	Index for sampling method.	
w_h^m	Weight of size group h of sampling method m .	
S	Sample size.	100, 200, ..., 1000
S_h^m	Sample size of size group h of sampling method m .	
k	Number of length classes.	40
L^m	Length composition data obtained by sampling method m .	

o_l^m	Samples at l - th length class, collected by sampling method m .	
π	Length composition rates of the total fish landed.	
μ	Mean of body length of fish landed.	10, 30, 50 cm
σ	Standard deviation of body length of fish landed.	20 cm
min	Minimum body length of fish landed.	10 cm
max	Maximum body length of fish landed.	50 cm
S1~S4	Scenarios for length distribution of total fish landed.	

2.3. Simulation experiments

I performed simulation experiments comparing the sampling methods ('current', 'proposal') to suggest a sampling method representing for the length composition rates of total fish landed. The simulation was conducted by imitating the actual sampling process. To imitate the actual sampling process, the sampling process was separated into landing, arrangement, and data collection steps in chronological order, and situations were assigned to each time step.

At landing time, I established four scenarios for the body length distribution of the total fish landed (Table 3.2). Three situations ($S1\sim S3$) assumed a truncated normal distribution, and one situation ($S4$) assumed a uniform distribution. The truncated normal distribution was used to limit the minimum and maximum values of the body length range of the fish landed. The number of individuals landed (C) involved two cases: 1 and 0.1 million for each length distribution scenario. For each scenario, each body length was generated with a constraint, where the minimum length was 10 cm and the maximum length was 50 cm, using the "truncnorm" package (Mersmann et al., 2018) and "seq" function in R. Each body weight of fish landed was generated with three parameters of a stochastic length-weight relationship. α and β were set as 0.003

$\text{g/cm}^{3.425}$ and 3.425 respectively. These values were taken from a study into chub mackerel (Gim, 2019). σ_w was set at 0.01 g.

At the arrangement time, it was assumed that all individuals landed were sorted into five body size groups according to the body length section of each size group, where length sections do not overlap between groups, and the width of the length section of all groups was 8 cm. Thus, five size groups were defined as follows: VSG: very small size group, (10cm, 18cm]; SG: small size group, (18cm, 26cm]; MG: medium size group, (26cm, 34cm]; LG: large size group, (34cm, 42cm]; VLG: very large size group, (42cm, 50cm]. Fish sorted by body size groups were placed into the boxes for each body size group with a weight of 18 kg, which is the weight of the fish in one box of chub mackerel (*Scomber japonicus*), as determined by the Busan Cooperative Fish Market in Korea.

At the data collection time, the simulated length data was collected by two sampling methods ('current', 'proposal') with sample sizes from 100 to 1,000 with an increment of 100. The simulated length composition data was obtained by discretizing with 40 length classes. The length classes were defined as follows: the width of each length class is 1cm, and the value of each length class is the midpoint value of the class: e.g., 10.5cm is the midpoint value of first length class, (10cm, 11cm].

For each sampling method, the simulation experiment was independently iterated 1,000 times, and each sampling method was evaluated using the estimates of length composition rates and their standard errors.

The estimates of the length composition rates obtained from 1,000 iterations of each sampling method were used to assess accuracy, by comparison with the true length composition rates. I also calculated the 95% coverage probability as the frequency at which the 95% confidence intervals of estimates of length composition rate contained the true length composition rates (Hyun et al., 2011). To calculate the 95% confidence intervals of estimates, I assumed that estimates followed the standard normal distribution. For example, the estimated 95% confidence interval for the l -th length composition rate from i -th iteration was equal to $\hat{\pi}_l^{(i)} \pm |z_{0.025}| \cdot SE(\hat{\pi}_l^{(i)})$, where $z_{0.025}$ is the 0.025th quantile of the standard normal variable (i.e., $z_{0.025} \cong -1.96$) and $SE(\hat{\pi}_l^{(i)})$ is standard error for the estimate $\hat{\pi}_l^{(i)}$. The 95% coverage probabilities of estimates of length compositions from the 1,000 iterations were displayed using boxplots, and then graphically compared between ‘current’ and ‘proposal’ sampling methods.

Table 3.2. Simulation scenarios of the length distribution of a population (i.e., a total of fish landed). Length distributions of all fish landed were generated under four scenarios with the assumption that the total of all fish landed was 0.1 and 1 million, respectively. μ and σ are the mean and the standard deviation of a truncated normal distribution. The shape of a length distribution differs by scenario: (1) *S1*: skewed to the right; (2) *S2*: symmetrical; (3) *S3*: skewed to the left; (4) *S4*: uniform.

Scenarios	Length distribution of Total fish landed
<i>S1</i>	Normal ($\mu = 10, \sigma = 20, \text{min} = 10, \text{max} = 50$)
<i>S2</i>	Normal ($\mu = 30, \sigma = 20, \text{min} = 10, \text{max} = 50$)
<i>S3</i>	Normal ($\mu = 50, \sigma = 20, \text{min} = 10, \text{max} = 50$)
<i>S4</i>	Uniform ($\text{min} = 10, \text{max} = 50$)

3. Results

In all body length distribution scenarios after the arrangement process, the ratios of boxes ($= w_h^{\text{Current}}$) and fish sorted ($= w_h^{\text{Proposal}}$) for each body size group were different (Table 3.3, Table 3.4). This result indicated that the number of samples for each body size group using the ‘current’ sampling method are not proportionate to the number of fish sorted for each body size group.

The estimates of the length composition rates obtained from the length composition data collected by the ‘current’ sampling method were clearly discriminated according to the length section of the five body size groups, and underestimated (negatively biased) for smaller length class values, but overestimated (positively biased) for larger length class values (second row of Fig. 3.2, and Fig. 3.3). The estimates in the ‘proposal’ sampling method accurately reflected the true value (third row of Fig. 3.2, and Fig. 3.3).

The 95% coverage probabilities of estimates of length compositions in the ‘current’ sampling method decreased as the sample size increased (gray colored boxplots in Fig. 3.4), while in the ‘proposal’ sampling method, the 95% coverage probabilities converged to 95% as the sample size increased in all body length classes (white colored boxplots in Fig.

3.4). However, in the *S4* scenario, in which the body length distribution of fish landed was assumed to be uniform, the 95% coverage probabilities of 200 samples were reduced compared to 100 samples.



Table 3.3. Sampling weights used by the current practice (w_h^{Current}) versus those used by the alternative practice (w_h^{Proposal}) set under each scenario when a total of all fish landed (C) was assumed to be 0.1 million. Five size groups are divided as follows: VSG: very small size group, (10cm, 18cm]; SG: small size group, (18cm, 26cm]; MG: medium size group, (26cm, 34cm]; LG: large size group, (34cm, 42cm]; VLG: very large group, (42cm, 50cm].

Scenarios		Body size groups (h)					Sum
		VSG	SG	MG	LG	VLG	
S1	Box_h	50	175	635	990	717	1,660
	w_h^{Current}	0.03	0.11	0.23	0.31	0.31	1
	C_h	32,443	28,008	20,230	12,564	6755	100,000
	w_h^{Proposal}	0.32	0.28	0.2	0.13	0.07	1

S2	Box_h	18	175	635	990	717	2,535
	$w_h^{Current}$	0.007	0.07	0.25	0.39	0.28	1
	C_h	9,807	23,983	32,672	24,011	9,527	100,000
	$w_h^{Proposal}$	0.1	0.24	0.33	0.24	0.1	1
S3	Box_h	12	91	405	1,201	2,633	4,342
	$w_h^{Current}$	0.003	0.02	0.09	0.28	0.6	1
	C_h	6,970	12,471	20,270	27,686	32,603	100,000
	$w_h^{Proposal}$	0.07	0.12	0.2	0.28	0.33	1

	Box_h	31	138	389	856	1,605	3,019
S4	w_h^{Current}	0.01	0.05	0.13	0.28	0.53	1
	C_h	20,000	20,000	20,000	20,000	20,000	100,000
	w_h^{Proposal}	0.2	0.2	0.2	0.2	0.2	1

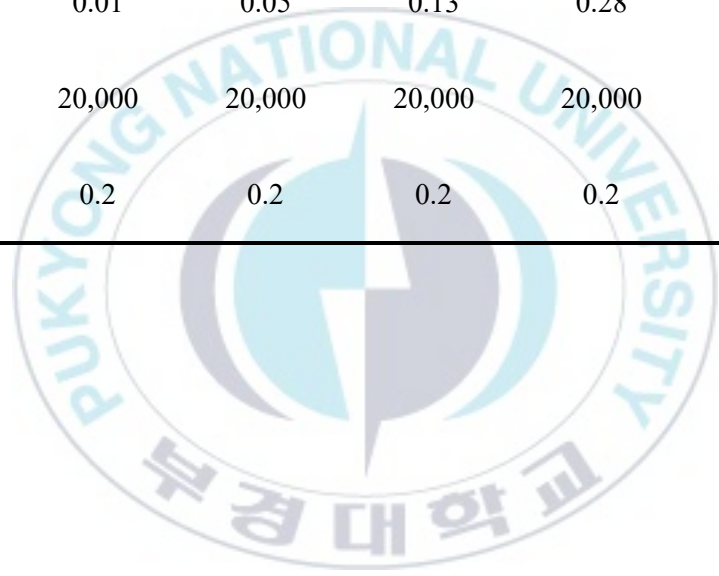
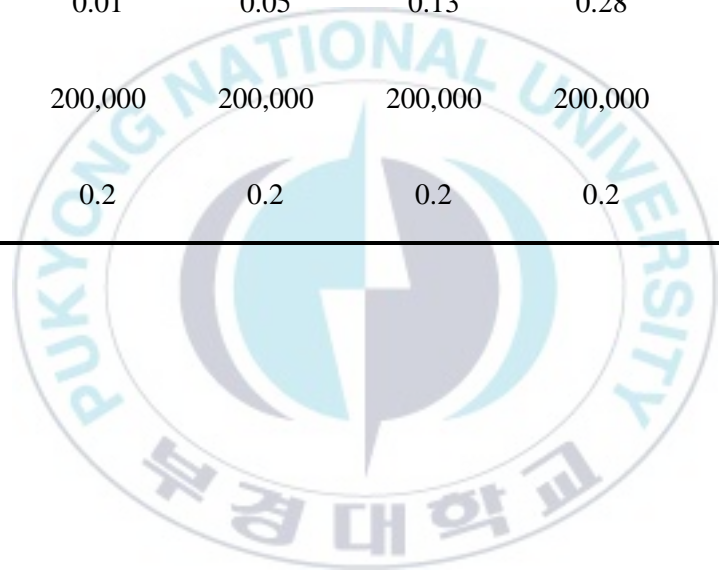


Table 3.4. Sampling weights used by the current practice (w_h^{Current}) versus those used by the alternative practice (w_h^{Proposal}) set under each scenario when a total of all fish landed (C) was assumed to be 1 million. Five size groups are divided as follows: VSG: very small size group, (10cm, 18cm]; SG: small size group, (18cm, 26cm]; MG: medium size group, (26cm, 34cm]; LG: large size group, (34cm, 42cm]; VLG: very large group, (42cm, 50cm].

Scenarios	Body size groups (h)					Sum	
	VSG	SG	MG	LG	VLG		
S1	Box_h	504	1,877	3,824	5,224	5,278	16,707
	w_h^{Current}	0.03	0.11	0.23	0.31	0.32	1
	C_h	325,324	278,086	202,467	126,125	67,998	1,000,000
	w_h^{Proposal}	0.33	0.28	0.20	0.13	0.07	1

S2	Box_h	180	1,768	6,335	9,907	7,300	25,490
	$w_h^{Current}$	0.01	0.07	0.25	0.39	0.29	1
	C_h	96,559	241,031	325,745	240,188	96,477	1,000,000
	$w_h^{Proposal}$	0.10	0.24	0.33	0.24	0.01	1
S3	Box_h	118	928	4,042	12,015	26,320	43,423
	$w_h^{Current}$	0.003	0.02	0.09	0.28	0.61	1
	C_h	67,812	127,281	201,799	276,917	326,191	1,000,000
	$w_h^{Proposal}$	0.07	0.13	0.20	0.28	0.33	1

	Box_h	313	1,382	3,893	8,562	16,063	30,213
S4	$w_h^{Current}$	0.01	0.05	0.13	0.28	0.53	1
	C_h	200,000	200,000	200,000	200,000	200,000	1,000,000
	$w_h^{Proposal}$	0.2	0.2	0.2	0.2	0.2	1



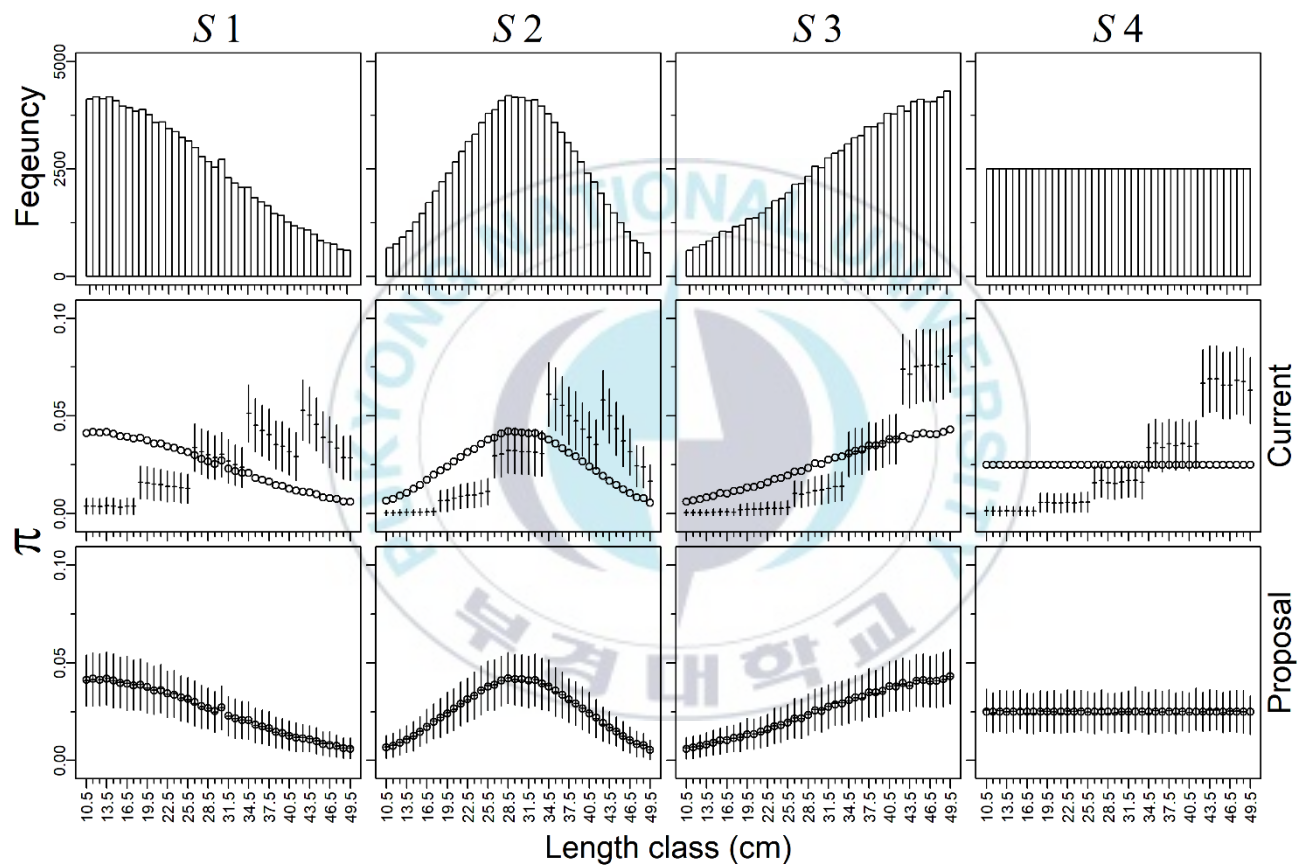
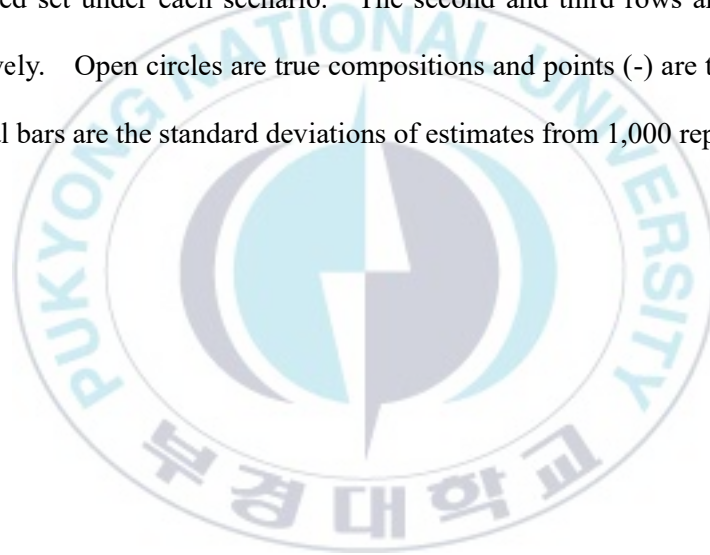


Fig. 3.2. Comparison in estimates ($\hat{\pi}$) of composition between the current and alternative practices with a sample size of 200 under four scenarios when a total of all fish landed (C) was 0.1 million individuals. The first row shows the length frequency of fish landed set under each scenario. The second and third rows are the results of current and alternative practices, respectively. Open circles are true compositions and points (-) are the mean values of estimates by length class and the vertical bars are the standard deviations of estimates from 1,000 replicates.



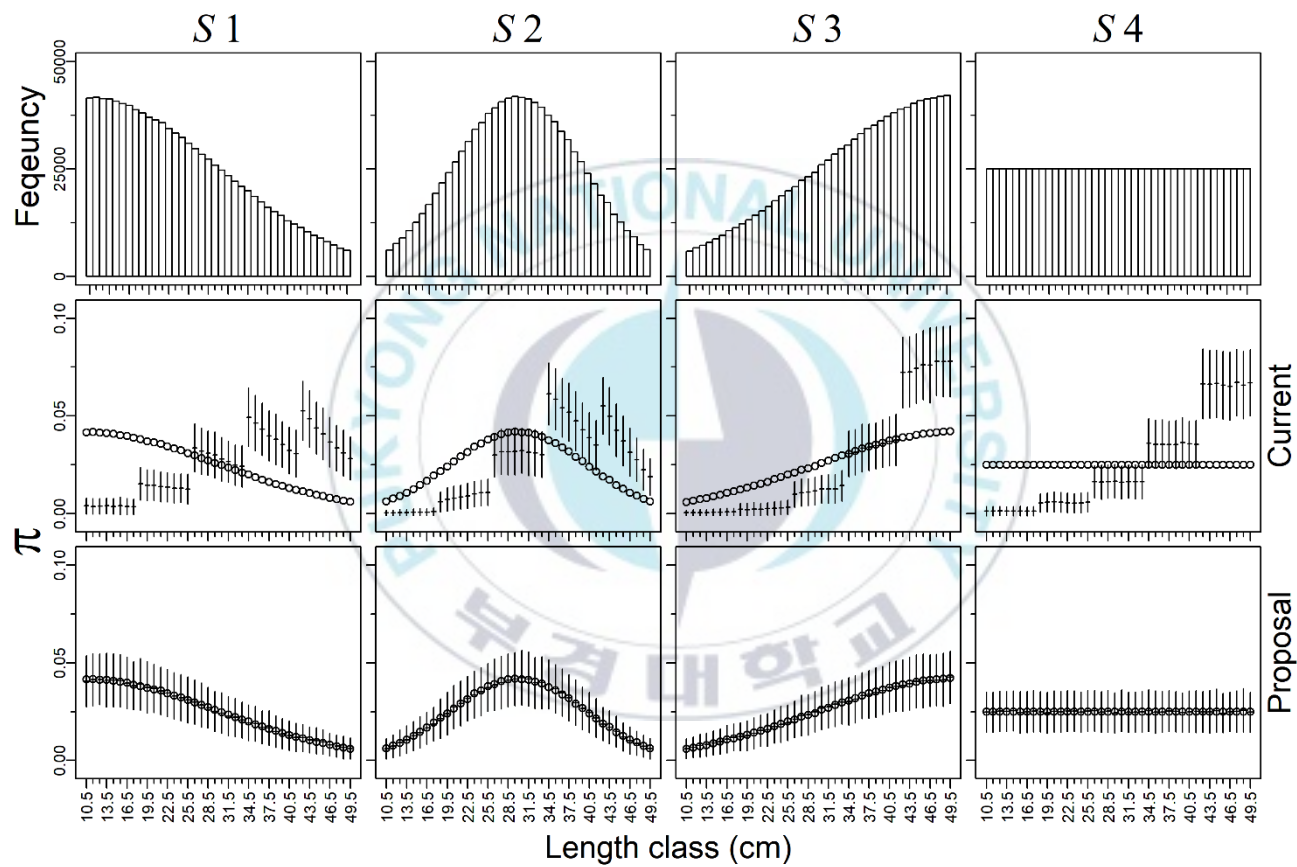
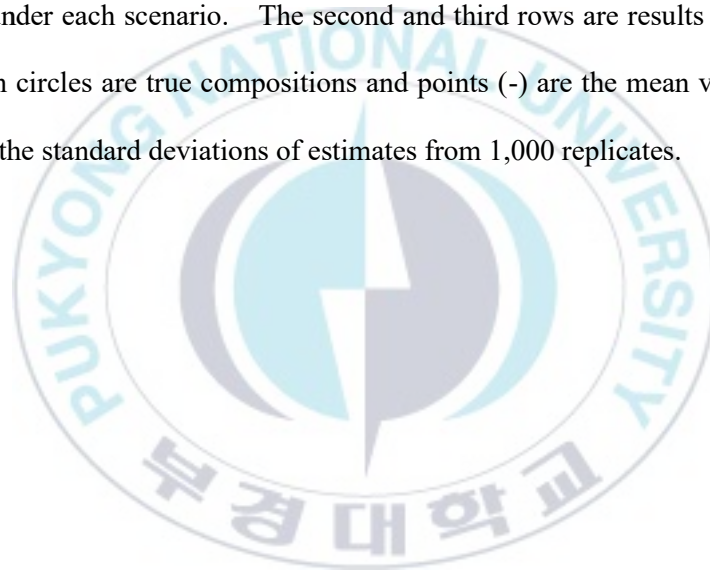


Fig. 3.3. Comparison in estimates ($\hat{\pi}$) of composition between the current and alternative practices with a sample size of 200 under four scenarios when a total of all fish landed (C) was 1 million individuals. The first row shows the length frequency of fish landed set under each scenario. The second and third rows are results from current and alternative practices, respectively. Open circles are true compositions and points (-) are the mean values of estimates by length class and the vertical bars are the standard deviations of estimates from 1,000 replicates.



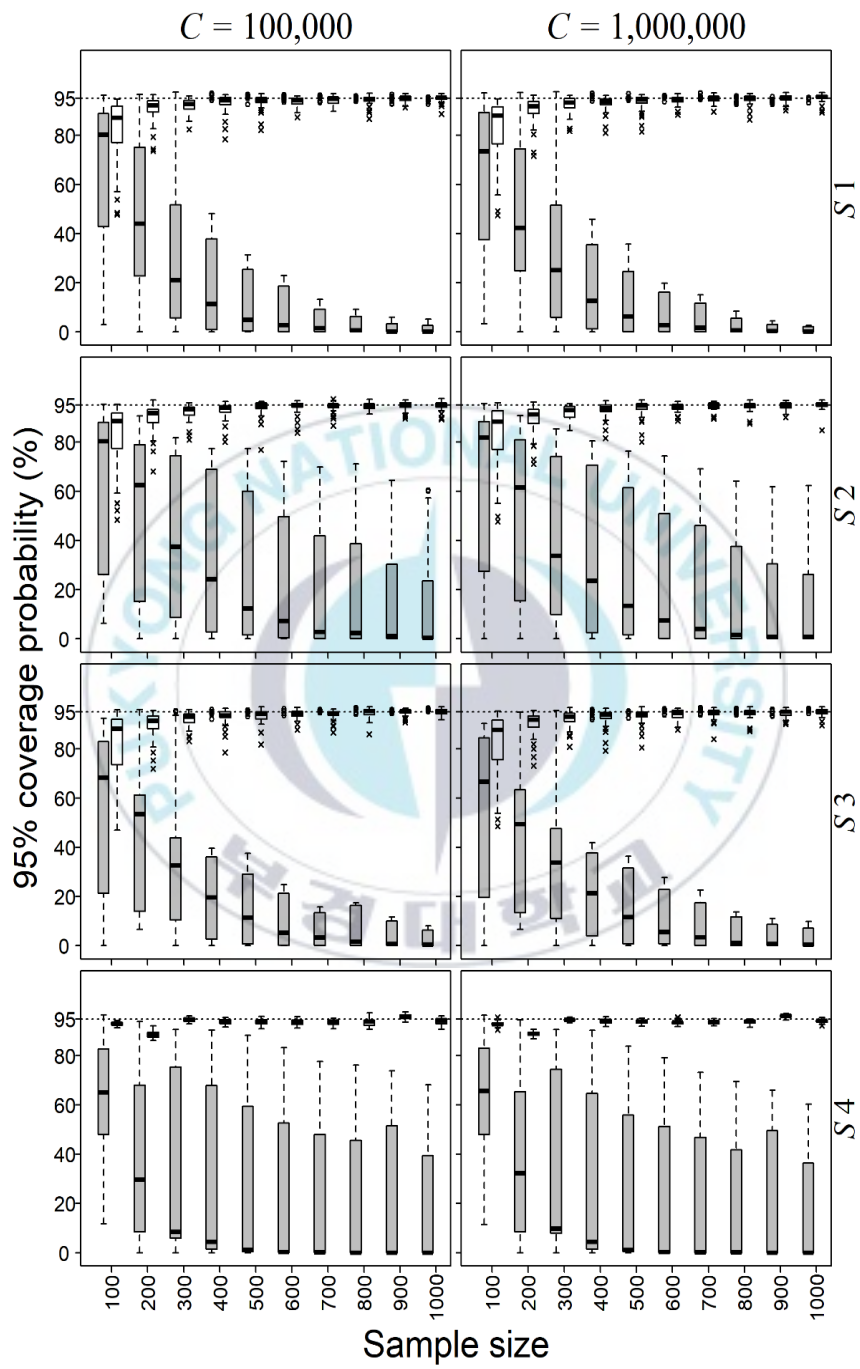
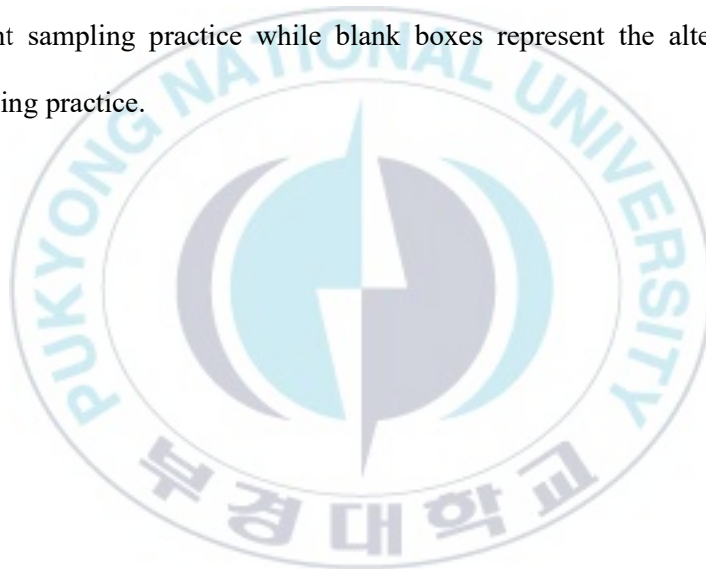


Fig. 3.4. Boxplots of 95% coverage probabilities of estimates of length compositions (i.e., 40 $\hat{\pi}$'s in the multinomial likelihood) by sample size considered. Simulation was performed for each of 10 cases of sample size (100, 200, ..., 1,000) under four scenarios by two cases of a total of fish landed ($C = 0.1$ million individuals under the left column; $C = 1$ million individuals under the right column). Gray boxes denote the current sampling practice while blank boxes represent the alternative sampling practice.



4. Discussion

The length composition data of fish sampled using the current method did not represent the length composition of the fish landed using simulation experiments. The estimates of length composition rates from the length composition data collected by the 'current' sampling method were clearly distinguished according to the body length section of body size groups, and smaller length classes were underestimated, but larger length class values were overestimated. This problem may arise because the compositions of the number of boxes are different from the composition of the number of fish sorted of body size groups. Since the 'current' sampling method uses sampling weights proportional to the number of boxes of body size groups, a large number of fish sorted are contained into one box in a small size group, but a small number of fish sorted are contained into one box in a large size group.

The 95% coverage probability was shown to be independent of the total number of fish landed, and to vary depending on the sample size and the shape of the length distribution of the fish landed. It was confirmed that the true composition rates were not included within the 95% confidence interval of the estimates from 'current' sampling method. The 'proposal' sampling method can represent the length composition of the fish landed.

But in the *S4* situation, in which the body length distribution of the fish landed is assumed to be uniform, the 95% coverage probability for 200 samples were decreased compared to that for 100 samples. This may be because the standard error of the estimates of length composition rates for the sample size of 100 is larger than that of the sample size of 200, so that the width of the 95% confidence interval where the sample size is 100 is wider than that of the sample size of 200.

In Korea, a process called arrangement is carried out before data are collected from fish landed, so there is a condition for performing stratified random sampling, in which sample data are collected for each body size group. However, manuals on sampling method or previous studies presenting representativeness of samples collected by the 'current' sampling method are insufficient. I performed simulation experiments to develop a sampling method. The 'current' sampling method using information on the number of boxes cannot represent the length composition of the fish landed, and as an alternative, it is suggested to use information on the number of fish landed. Thus, it is necessary to pay attention to the arrangement process of the catch before data is collected, and it is suggested to investigate the number of fish sorted by body size group.

Conclusions

In this study, I developed a length-based assessment model for the common squid in multiple fisheries, and applied the model to actual data sets. However, I found that length composition data, which are the key data of my model, did not represent the length composition of fish landed. Assessment results using actual data sets therefore cannot be presented as representative of the common squid population. As an alternative, I evaluated the model by performing simulation experiments. The model was able to provide the parameter estimates including body growth parameters, fishing and natural mortality, population size, reproduction rate, gear selectivity parameters, and length-weight relationship parameters, but my model still confronted problems of estimation for a parameter related to migration, and the assumption of independence between length compositions (multinomial variables) and yields (lognormal variable). Therefore, further studies on migration of the common squid and correlation between length compositions and yields should be performed.

Acknowledgements

This study was financially supported by the Korean National Institute of Fisheries Science (NIFS) under project No. R2020022 and the National Research Foundation of Korea (NRF) under project No. NRF-2019R1I1A2A01052106. Data were provided by the NIFS, the Statistics Korea, and Kim et al (1997).

I am hereby express my sincere gratitude to my thesis advisor Prof. Saang-Yoon Hyun. Without his dedicated guidance, advice, and teaching, this thesis could not be completed. I also thank Yeonghye Kim, Jung Jin Kim, Ken Mori, Toshiki Kaga, Dongyoung An, Busan Cooperative Fish Market, and Korea Fisheries Resources Agency for advice and support in the progress of this project.

References

- Baranov, F.I., 1945, *On the question of the biological basis of fisheries ; On the question of the dynamics of the fishing industry*, Indiana University, Bloomington, Ind.
- BCFM (Busan Cooperative Fish Market). 2020. Website for fishery consignment sales in Busan Cooperative Fish Market. Retrieved from http://www.bcfm.co.kr/sub/order_01.jsp.
- Beverton, R.J.H. and Holt, S.J. (1957) *On the Dynamics of Exploited Fish Populations*. London: Chapman and Hall (facsimile reprint, 1993), 533 pp.
- Branch, T.A. 2009, "Differences in predicted catch composition between two widely used catch equation formulations", *Canadian Journal of Fisheries and Aquatic Sciences*, vol. 66, no. 1, pp. 126-132.
- Cohen, M. & Fishman, G.S. 1980, "Modeling Growth–Time and Weight–Length Relationships in a Single Year-Class Fishery with Examples for North Carolina Pink and Brown Shrimp", *Canadian Journal of Fisheries and Aquatic Sciences*, vol. 37, no. 6, pp. 1000-1011.
- Deriso, R.B. & Parma, A.M. 1988, "Dynamics of Age and Size for a Stochastic Population Model", *Canadian Journal of Fisheries and Aquatic Sciences*, vol. 45, no. 6, pp. 1054-1068.

- Francis, R.I.C.C. 2011, "Data weighting in statistical fisheries stock assessment models", *Canadian Journal of Fisheries and Aquatic Sciences*, vol. 68, no. 6, pp. 1124-1138.
- Fries, A.S. 2010, "A Gap Analysis of the Distributions of Cephalopod Species Worldwide with a Focus on Commercially Important Species", .
- Fu, C. & Quinn II, T.J. 2000, "Estimability of natural mortality and other population parameters in a length-based model: *Pandalus borealis* in Kachemak Bay, Alaska", *Canadian Journal of Fisheries and Aquatic Sciences*, vol. 57, no. 12, pp. 2420-2432.
- Gim J. 2019. "A length-based model for Korean chub mackerel (*Scomber japonicus*) stock". MS. Thesis. Pukyong National University. Korea.
- Hyun, S., Reynolds, J. & Galbreath, P. 2011, "Accounting for Tag Loss and Its Uncertainty in a Mark-Recapture Study with a Mixture of Single and Double Tags", *Transactions of the American Fisheries Society*, vol. 141, pp. 11-25.
- Jo M. J., Kim J. J., Yang J. H., Kim C. S., Kang S. K. 2019, "Changes in the Ecological Characteristics of *Todarodes pacificus* associated with Lon-term Catch Variations in Jigging Fishery", *Korean Society of Fisheries*, vol. 52, no. 6, pp. 685-695.

- Kidokoro H. 2010, "Forecasting methods on the fishing conditions of Japanese common squid in the Sea of Japan". *Report of the 2009 Annual Meeting and Squid Resources*. 3-12 (in Japanese).
- Kim J. J., Lee H. H., Kim S., Park C. 2011, "Distribution of Larvae of the Common Squid *Todarodes paificus* in the Northern East China Sea", *Korean Society of Fisheries*, vol. 44, no. 3, pp. 267-275.
- Kim Y. H. & Kang Y. J. 1995, "Population Analysis of the Common Squid, *Todarodes pacificus* Steenstrup in Korean Waters -1. Separation of Population-", *Korean Journal of Fisheries and Aquatic Sciences*, vol. 28.
- Kim Y. H., Kang Y. J., Choi S. H., Park C. S., Baik C.I. 1997, "Population Analysis by the Reproductive Ecological Method for the Common squid, *Todarodes pacificus* in Korean Waters", *Korean Society of Fisheries*, vol. 30, no. 4, pp. 523-527.
- Kristensen, K., Nielsen, A., Berg, C., Skaug, H. & Bell, B. 2016, "TMB: Automatic Differentiation and Laplace Approximation", *Journal of Statistical Software, Articles*, vol. 70, no. 5, pp. 1-21.
- Lohr S. L. 1998. *Sampling: Design and analysis*. Julet M, ed. Brooks/Cole, Boston, MA, U.S.A., 73-82.
- Lorenzen, K. 1996, "The relationship between body weight and natural mortality in juvenile and adult fish: a comparison of natural

ecosystems and aquaculture", *Journal of fish biology*, vol. 49, no. 4, pp. 627-642.

Mark M., Baurzhan M., Tobias W., Alexander W., Bas S. badshah400 and Mo-Gul and The Gitter Badger and Zbigniew Jędrzejewski-Szmek and kensington and kylesower 2020, "markummitchell/engauge-digitizer: Nonrelease", .

Mersmann, O., Trautmann, H., Steuer, D. & Bornkamp, B. 2018, *truncnorm: Truncated Normal Distribution*, .

Miller, T.J. & Hyun, S. 2018, "Evaluating evidence for alternative natural mortality and process error assumptions using a state-space, age-structured assessment model", *Canadian Journal of Fisheries and Aquatic Sciences*, vol. 75, no. 5, pp. 691-703.

Nakamura, Y. 1993, "Age determination from daily growth increments in statoliths of some groups of the Japanese common squid *Todarodes pacificus*", *Recent Advances in Cephalopod Fisheries Biology*, , pp. 337-342.

NFRDI (National Fisheries Research and Development Institute) & PKNU (Pukyong National University) 2004, *Fisheries resources research techniques*, National Fisheries Research and Development Institute Fisheries Resources Department Fisheries Resources Research Team, Korea

NOAA (National Oceanic and Atmospheric Administration). 2020.

Website for sock assessment model description. Retrieved from <https://www.fisheries.noaa.gov/insight/stock-assessment-model-descriptions>.

Punt, A.E. 2003, "Extending production models to include process error in the population dynamics", *Canadian Journal of Fisheries and Aquatic Sciences*, vol. 60, no. 10, pp. 1217-1228.

Punt, A.E., Huang, T. & Maunder, M.N. 2013, "Review of integrated size-structured models for stock assessment of hard-to-age crustacean and mollusc species", *ICES Journal of Marine Science*, vol. 70, no. 1, pp. 16-33.

Quinn, T., Turnbull, C. & Fu, C. 1998, "A Length-Based Population Model for Hard-to-Age Invertebrate Populations", .

R Core Team. 2020. R: a language and environment for statistical computing. R Foundation for Statistical Computing, Vienna, Austria. Retrieved from <http://www.R-project.org/>.

Ricker, W.E. 1954, "Stock and Recruitment", *Journal of the Fisheries Research Board of Canada*, vol. 11, no. 5, pp. 559-623.

Sakurai, Y., Kiyofuji, H., Saitoh, S., Goto, T. & Hiyama, Y. 2000, "Changes in inferred spawning areas of *Todarodes pacificus* (Cephalopoda: Ommastrephidae) due to changing environmental

conditions", *ICES Journal of Marine Science*, vol. 57, no. 1, pp. 24-30.

Sakurai, Y., Kidokoro, H., Yamashita, N., Yamamoto, J., Uchikawa, K. & Takahara, H. 2013, "*Todarodes pacificus*, Japanese common squid", *Advances in Squid Biology, Ecology and Fisheries. Part II - Oegopsid squids*, , pp. 249-271.

Scheaffer R.L., Mendenhall W., Ott R.L. and Gerow K.G. 1971. *Elementary survey sampling*, Julet M, ed. Brooks/Cole, Boston, MA, U.S.A., 114-133.

SeaLifeBase. 2020, Website for biological information in SeaLifeBase. Retrieved from <https://www.sealifebase.se/summary/Todarodes-pacificus.html>.

Sugawara, M., Yamashita, N., Sakaguchi, K., Sato, T., Sawamura, M., Yasue, N., Mori, K. & Fukuwaka, M. 2013, "Effects of hatch timing and sex on growth of the winter-spawning stock of Japanese common squid *Todarodes pacificus* migrating in the Pacific Ocean", *NIPPON SUISAN GAKKAISHI*, vol. 79, no. 5, pp. 823-831.

Tjørve, Kathleen M. C. AND Tjørve, Even 2017, "The use of Gompertz models in growth analyses, and new Gompertz-model approach: An addition to the Unified-Richards family", *PLOS ONE*, vol. 12, no. 6, pp. 1-17.

Appendix 1. Derivation of expected length and variance of aged individual.

Consider the deterministic Gompertz growth model as

$$L_a = L_\infty \cdot \exp\left[-\exp(-G \cdot (a - a_0))\right] \quad (1)$$

From equation (1), length at age $a+1$ can be transformed by length at age a :

$$\begin{aligned} L_{a+1} &= L_\infty \cdot \exp\left[-\exp(-G \cdot (a+1 - a_0))\right] \\ &= L_\infty \cdot \exp\left[-\exp(-G) \cdot \exp(-G \cdot (a - a_0))\right] \end{aligned} \quad (2)$$

Taking the natural logarithm of both sides of equation (2):

$$\begin{aligned} \log L_{a+1} &= \log L_\infty - \exp(-G) \cdot \exp(-G \cdot (a - a_0)) \\ &= \log L_\infty - \exp(-G) \cdot \log\left(\frac{L_a}{L_\infty}\right) \end{aligned} \quad (3)$$

Exponentiate both sides of equation (3) and then L_{a+1} is function of L_a (i.e., the length of an aged individual is explained by previous length).

$$L_{a+1} = L_{\infty} \cdot \left(\frac{L_a}{L_{\infty}} \right)^{\rho} ; \rho = \exp[-G] \quad (4)$$

Then, assume a multiplicative error model:

$$L_{a+1} = L_{\infty} \cdot \left(\frac{L_a}{L_{\infty}} \right)^{\rho} \cdot e^{\varepsilon_{a+1}} ; \varepsilon_{a+1} \sim N(0, \sigma_G^2) \quad (5)$$

Expected value of equation (5) is

$$E[L_{a+1}] = L_{\infty} \cdot \left(\frac{L_a}{L_{\infty}} \right)^{\rho} \cdot \exp\left[\frac{\sigma_G^2}{2} \right] \quad (6)$$

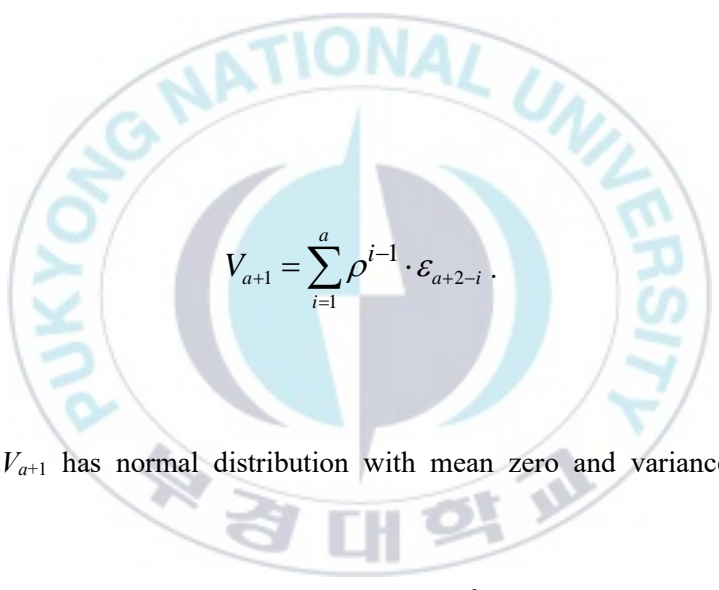
From equation (5) and an assumption that length at age r (= age 1) is normally distributed with mean μ_r and variance σ_r^2 , length at age $a+1$ is modified as:

$$L_{a+1} = L_{\infty} \cdot \left(\frac{L_{a=1}}{L_{\infty}} \right)^{\rho} \cdot \exp\left[\sum_{i=1}^a \rho^{i-1} \cdot \varepsilon_{a+2-i} \right]. \quad (7)$$

Taking the natural logarithm of both sides of equation leads to

$$\log L_{a+1} = (1 - \rho^a) \cdot \log L_\infty + \rho^a \cdot \log L_1 + V_{a+1}, \quad (8)$$

where


$$V_{a+1} = \sum_{i=1}^a \rho^{i-1} \cdot \varepsilon_{a+2-i}.$$

Here V_{a+1} has normal distribution with mean zero and variance

$$\text{Var}[V_{a+1}] = \sigma_G^2 \cdot \frac{1 - \rho^{2a}}{1 - \rho^2} \quad (9)$$

Thus, $\log L_{a+1}$ is normally distributed with mean

$$\begin{aligned}
E[\log L_{a+1}] &= (1 - \rho^a) \cdot \log L_\infty + \rho^a \cdot E[\log L_1] + E[V_{a+1}] \\
&= (1 - \rho^a) \cdot \log L_\infty + \rho^a \cdot E\left[\log \mu_r + \frac{(L_1 - \mu_r)}{\mu_r} - \frac{(L_1 - \mu_r)^2}{2 \cdot \mu_r^2}\right], \quad (10) \\
&= (1 - \rho^a) \cdot \log L_\infty + \rho^a \cdot \left[\log \mu_r - \frac{\sigma_r^2}{2 \cdot \mu_r^2}\right]
\end{aligned}$$

and variance

$$\begin{aligned}
\text{Var}[\log L_{a+1}] &= \rho^{2a} \cdot \text{Var}[\log L_1] + \text{Var}[V_{a+1}] \\
&= \rho^{2a} \cdot \text{Var}\left[\log \mu_r + \frac{(L_1 - \mu_r)}{\mu_r}\right] + \sigma_G^2 \cdot \frac{1 - \rho^{2a}}{1 - \rho^2}. \quad (11) \\
&= \rho^{2a} \cdot \frac{\sigma_r^2}{\mu_r^2} + \sigma_G^2 \cdot \frac{1 - \rho^{2a}}{1 - \rho^2}
\end{aligned}$$

Here, $E[\log L_1]$ and $\text{Var}[\log L_1]$ are obtained approximately by using the delta method. Then, the variance of L_{a+1} is given as

$$\text{Var}[L_{a+1}] = \left(e^{\text{Var}[\log L_{a+1}]} - 1\right) \cdot e^{2 \cdot E[\log L_{a+1}] + \text{Var}[\log L_{a+1}]}. \quad (12)$$

Appendix 2. TMB code for the length-based assessment model for the common squid.

CPP file

```
#include <TMB.hpp>

// pass missing values
template<class Type>
bool isNA(Type x){
    return R_IsNA(asDouble(x));
}

// square
template<class Type>
Type square(Type i) {
    return i*i;
}

//objective function
template<class Type>
Type objective_function<Type>::operator() () {

    // DATA SECTION;
    DATA_INTEGER(Plus_switch); // Switch for the last age class
    (0: Maximum age, "A"; 1: Terminal age, "A+");
    DATA_INTEGER(JIG_Sel_switch); // Switch for the size-specific
    gear selectivity of jigger fishery (0: logistic; 1: Gamma; 2:
    lognormal);
    DATA_INTEGER(nages); // nages: number of age classes by
    TWO-month;
    DATA_INTEGER(nlengths); // nlengths: number of length
    classes; 0.5, 11.5, ... , 33.5 (cm);
    DATA_INTEGER(nmos); // nmos: number of TWO-months for
```

the fishery catch data: 2016. 05&06 ~ 2018. 11&12;

```
// Input parameters;
DATA_SCALAR(mu_r); // the mean (cm) of the lengths at the
recruit stage: i.e., age 1 = 1 two-months. mu_r = 1.47 cm
(Sugawara et al., 2013);
DATA_SCALAR(Linf); // Linf: asymptotic length = 33.7 cm
(Sugawara et al., 2013);
DATA_SCALAR(b1); // b1: a parameter in weight-natural
mortality (Lorenzen, 1996);
DATA_SCALAR(Sex_r_female); // Sex_r_female: sex ratio at
the recruit stage, Sex_r_female = (1-Sex_r_male) = 0.5;
// beta_0 & beta_1: parameters in mantle length (cm)-maturation
(Jo et al., 2019);
DATA_SCALAR(beta_0);
DATA_SCALAR(beta_1);

// Actual data;
DATA_VECTOR(Year); // 2016 ~ 2018;
DATA_VECTOR(MONTH); // 5&6.2016 ~ 11&12.2018;
DATA_VECTOR(JIG_CPUE); // CPUE (MT/hook) from jigger
fisheries;
DATA_VECTOR(JIG_yield); // Yield (MT) from jigger fisheries;
DATA_VECTOR(PS_CPUE); // CPUE (MT/haul) from large
purse-seine fisheries;
DATA_VECTOR(PS_yield); // Yield (MT) from large purse-seine
fisheries;
DATA_VECTOR(Total_yield); // Yield (MT) from all fisheries;
DATA_VECTOR(x); // 34 length classes: 0.5cm, 1.5cm, ..., 33.5
cm;
DATA_VECTOR(Wighting_para); // Wighting_para: weighting
term for each likelihood component;
DATA_VECTOR(lengthAL); // Mantle lengths (cm) in length-
weight data;
DATA_VECTOR(weightAL); // Body weight (g) in length-weight
data;
```

```

DATA_VECTOR(lengthFC); // Mantle lengths (cm) in length-
weight data;
DATA_VECTOR(EggFC); // Mantle lengths (cm) in length-
weight data;

DATA_MATRIX(JIG_length_compo); // Length composition data
from jigger fisheries;
DATA_MATRIX(PS_length_compo); // Length composition data
from large purse-seine fisheries;

// std::cout << " !! DATA FINISH !! " << std::endl;

// PARAMETER SECTION;
PARAMETER(log_sig2_r); // Log-scaled variance (log (cm^2))
of the lengths at the recruit stage;
PARAMETER(log_G); // Log-scaled instantaneous growth rate
in Gompertz growth model;
PARAMETER(log_sigma_G); // Log-scaled variance (cm^2) in
stochastic Gompertz growth model;
PARAMETER(JIG_log_q); // Log-scaled catchability of jigger
fisheries;
PARAMETER(PS_log_q); // Log-scaled catchability of large
purse-seine fisheries;
PARAMETER(JIG_gamma); // Catchability of jigger fisheries;
PARAMETER(PS_gamma); // Catchability of large purse-seine
fisheries;
PARAMETER(JIG_log_L50); // Log-scaled length of fish when
the fish encountered the jigger fishery is caught with 50%
probability;
PARAMETER(PS_log_L50); // Log-scaled length of fish when
the fish encountered the large purse-seine fishery is caught with 50%
probability;
PARAMETER(log_TO_F_init); // Log-scaled instantaneous
fishing mortality rate of the others at initial time (5&6. 2016);
PARAMETER_VECTOR(log_F_TO); // Log-scaled
instantaneous fishing mortality rate of the others at time '2' (5&6.

```

```

2016) ~ '16' (11&12. 2018);
    PARAMETER_VECTOR(log_N_init); // Log-scaled the number
of individuals of age '1' ~ '6+' at initial time;
    PARAMETER(log_Pi_5); // Log-scaled arrival rate at spawning
ground of a cohort of age 5;
    PARAMETER(log_b0); // Log-scaled parameter in weight-
natural mortality (Lorenzen, 1996);
    // log_aWL & log_bWL: log-scaled parameters in mantle length
(cm)-body weight (g);
    PARAMETER(log_aWL);
    PARAMETER(log_bWL);
    // log_aFC & log_bFC: log-scaled parameters in mantle length
(cm)-Eggs (No.);
    PARAMETER(log_aFC); // Fixed by using mapped in
MakeADFun;
    PARAMETER(log_bFC); // Fixed by using mapped in
MakeADFun;

    // std::cout << " !! PARAMETERS FINISH !! " << std::endl;

// PRELIMINARY SECTION;

//Derived quantities;
int ncohorts = nmos;
int nAL = lengthAL.size();
int nFC = EggFC.size();

    vector<Type> TO_yield = Total_yield-(JIG_yield+PS_yield); //
Yield (MT) of the others;
    vector<Type> JIG_effort = JIG_yield/JIG_CPUE; // Effort (hooks)
of jigger fisheries;
    vector<Type> PS_effort = PS_yield/PS_CPUE; // Effort (hauls)
of large purse-seine fisheries;
    vector<Type> L = x; // The length classes after one growth
increment;

```

```

// Exponentiate the free parameters;
Type Pi_5 = exp(log_Pi_5);
Type sig2_r = exp(log_sig2_r);
Type JIG_q = exp(JIG_log_q);
Type PS_q = exp(PS_log_q);
Type JIG_L50 = exp(JIG_log_L50);
Type PS_L50 = exp(PS_log_L50);
Type b0 = exp(log_b0);
Type G = exp(log_G);
Type Rho = exp(-Type(1.0)*G);
Type sigma_G = exp(log_sigma_G);
Type aWL = exp(log_aWL);
Type bWL = exp(log_bWL);
Type aFC = exp(log_aFC);
Type bFC = exp(log_bFC);
vector<Type> N_init = exp(log_N_init);

// Length class (cm) - body weight (kg);
vector<Type> Wt(nlengths);
Wt.setZero();
Wt = aWL*pow(x,bWL)/Type(1000); // !! "/Type(1000)" makes
dimension (g) convert to dimension (kg);

// Length class (cm) - Eggs (No.);
vector<Type> fecundity(nlengths);
fecundity.setZero();
fecundity = aFC*pow(x,bFC);

// Instantaneous fishing mortality rates for each fishery;
vector<Type> JIG_F(nmos);
vector<Type> PS_F(nmos);
vector<Type> TO_F(nmos);
// Size- and time- specific fishing mortality rates for each fishery;
matrix<Type> JIG_F_tx(nmos,nlengths);
matrix<Type> PS_F_tx(nmos,nlengths);
matrix<Type> TO_F_tx(nmos,nlengths);

```

```

matrix<Type> Z(nmos,nlengths); // Total mortality rate;
matrix<Type> ExpZ(nmos,nlengths); // Survival rate;

// Body growth;
matrix<Type> f(nages,nlengths); // Probability mass function of
length distribution at each age;
vector<Type> Mu(nlengths); // Expected length after growth
increment for an individual of the length class 'x';
vector<Type> SS(nages); // Variance of the length distribution at
age 'a+1' after growth for an individual of the length class 'x' at age
'a';
vector<Type> Mean_logN_L(nages); // Expected value of length
at age 'a+1';
vector<Type> Var_logN_L(nages); // Variance of length at age
'a+1';
array<Type> pp(nlengths,nlengths,nages); // Conditional
probability of individuals at the length class 'l' after one growth
increment for an individual at the length class 'x';

// Abundance;
vector<Type> p(nlengths); // Relative distribution of lengths of a
cohort at age 'a' at the beginning of time 't' after the processes of
mortality and growth;
vector<Type> N_plus(nmos+1); // Survived individuals from
terminal age after mortality;
matrix<Type> N(nages,nmos+2); // Number of individuals at the
beginning of time 't';
matrix<Type> Nx(nmos+1,nlengths); // Number of individuals at
length class 'x';
array<Type> NL(ncohorts+1,nlengths,nages); // Number of
individuals at length class 'x' of age 'a' at the beginning of time 't';

// Females;
vector<Type> F_p(nlengths); // Relative distribution of lengths of
a female cohort at age 'a' at the beginning of time 't' after the

```

```

processes of mortality and growth;
  vector<Type> F_p_plus(nlengths); // Relative distribution of
lengths of a female cohort of terminal age at the beginning of time
't' after the processes of mortality and growth;
  matrix<Type> F_N(nages,nmos+1);
  matrix<Type> F_f(nages,nlengths); // Probability of female
individuals at the length class 'x' of a cohort, with age 'a' at the
beginning of time 't';
  matrix<Type> F_f_init(nages,nlengths); // Probability of female
individuals at the length class 'x' of a cohort, with age 'a' at the
beginning of initial time;
  array<Type> F_NL(ncohorts+1,nlengths,nages);

// Males;
  vector<Type> M_p(nlengths); // Relative distribution of lengths
of a male cohort at age 'a' at the beginning of time 't' after the
processes of mortality and growth;
  vector<Type> M_p_plus(nlengths); // Relative distribution of
lengths of a male cohort of terminal age at the beginning of time 't'
after the processes of mortality and growth;
  matrix<Type> M_N(nages,nmos+1);
  matrix<Type> M_f(nages,nlengths); // Probability of male
individuals at the length class 'x' of a cohort, with age 'a' at the
beginning of time 't';
  matrix<Type> M_f_init(nages,nlengths); // Probability of male
individuals at the length class 'x' of a cohort, with age 'a' at the
beginning of initial time;
  array<Type> M_NL(ncohorts+1,nlengths,nages);

// Spawning;
  vector<Type> ARRIVE(nages); // Arrival rates at age 'a';
  vector<Type> Eggs(nmos+1); // Number of eggs at time 't';
  vector<Type> Sex_A_init(nages); // Female ratio of age 'a' at the
beginning of initial time;
  vector<Type> maturation(nlengths); // Length class (cm)-
maturation;

```

```

    maturation = Type(1.0)/(Type(1.0)+exp(beta_0+beta_1*x));
    matrix<Type> Sex_A(nages,nmos+1); // Female ratio of age 'a'
at the beginning of time 't';
    matrix<Type> Spawners(nages,nmos+1); // Number of
spawners of age 'a' at the beginning of time 't';
    array<Type> SpawnersL(ncohorts+1,nlengths,nages); //
Number of spawners at length class 'l' of age 'a' at the beginning
of time 't';

// Catch & Yield & Biomass;
matrix<Type> JIG_Catch(nmos,nlengths);
matrix<Type> PS_Catch(nmos,nlengths);
matrix<Type> TO_Catch(nmos,nlengths);
vector<Type> JIG_Yieldhat(nmos);
vector<Type> PS_Yieldhat(nmos);
vector<Type> TO_Yieldhat(nmos);
vector<Type> B(nmos+1);
vector<Type> Pop(nmos+1);
matrix<Type> JIG_LF(nmos,nlengths);
matrix<Type> PS_LF(nmos,nlengths);
vector<Type> JIG_SamSize(nmos);
vector<Type> PS_SamSize(nmos);

// Objective function;
vector<Type> nll(8); // Likelihood component (Negative Log-
Likelihood);
vector<Type> RSS(7); // RSS: Residual Sum of Squares;

// std::cout << " !! PRELIMINARY CALCULATION FINISH !! "<<
std::endl;

// PROCEDURE SECTION;

// Mortality process;
// Selectivity for each fishery;
// jigger fishery;

```

```

vector<Type> JIG_Sel(nlengths);
if(JIG_Sel_switch == 0) { // logistic;
    JIG_Sel = Type(1.0)/(Type(1.0)+exp(Type(-
1.0)*JIG_gamma*(x-JIG_L50)));
} else if(JIG_Sel_switch == 1) { // Gamma;
    Type shape = 1/(JIG_gamma*JIG_gamma); //
JIG_gamma=CV;
    Type rate = (shape-1)/JIG_L50; // JIG_L50=mode;
    for(int i=0;i<nlengths;i++) {
        JIG_Sel(i) =
(pow(rate,shape))*(1/exp(lgamma(shape)))*(pow(x(i),(shape-
1)))*(exp(-rate*x(i)));
    };
    JIG_Sel /= max(JIG_Sel);
} else if(JIG_Sel_switch == 2){ // lognormal;
    Type log_sd = sqrt(log(JIG_gamma*JIG_gamma+1));
    Type log_mean = log(JIG_L50)+log_sd*log_sd;
    for(int i=0;i<nlengths;i++) {
        JIG_Sel(i) = (1/(x(i)*log_sd*sqrt(2*PI)))*exp(-((log(x(i))-
log_mean)*(log(x(i))-log_mean)/(2*log_sd*log_sd));
    };
    JIG_Sel /= max(JIG_Sel);
};
// large purse-seine fishery;
vector<Type> PS_Sel = Type(1.0)/(Type(1.0)+exp(Type(-
1.0)*PS_gamma*(x-PS_L50))); // logistic;
// the others;
vector<Type> TO_Sel(nlengths); // not assumed;
for(int xind=0;xind<nlengths;xind++) {
    TO_Sel(xind) = Type(1.0);
};

// Instantaneous fishing Mortality;
JIG_F.setZero();
PS_F.setZero();
TO_F.setZero();

```

```

for(int t=0;t<nmos;t++) {
    JIG_F(t) = JIG_q*JIG_effort(t); // F = q*Effort;
    PS_F(t) = PS_q*PS_effort(t); // F = q*Effort;
    if(t == 0) {
        TO_F(t) = exp(log_TO_F_init); // random-walk model;
    } else if(t > 0) {
        TO_F(t) = exp(log_F_TO(t-1)); //TO_F(t-
1)*exp(TO_dev(t-1));
    };
};

// Natural Mortality (modified from Lorenzen (1996));
vector<Type> M = b0*pow(aWL,Type(-1.0)*b1)*pow(x,Type(-
1.0)*b1*bWL);

// Total Mortality & Survival rate;
JIG_F_tx.setZero();
PS_F_tx.setZero();
TO_F_tx.setZero();
Z.setZero();
ExpZ.setZero();
for(int t=0;t<nmos;t++)
    for(int xind=0;xind<nlengths;xind++) {
        JIG_F_tx(t,xind) = JIG_F(t)*JIG_Sel(xind);
        PS_F_tx(t,xind) = PS_F(t)*PS_Sel(xind);
        TO_F_tx(t,xind) = TO_F(t)*TO_Sel(xind);

        Z(t,xind) =
M(xind)+JIG_F_tx(t,xind)+PS_F_tx(t,xind)+TO_F_tx(t,xind);
        ExpZ(t,xind) = exp(Type(-1.0)*Z(t,xind));
    };
//std::cout << " !! MORTALITY PROCESS FINISH !! " << std::endl;

// Growth process (Gompertz);
Type kkk = Type(0.0);
SS(0) = sig2_r;

```

```

f.row(0) =
dnorm(x,mu_r,sqrt(SS(0)))/sum(dnorm(x,mu_r,sqrt(SS(0))));

Mu = Linf*(pow((x/Linf),Rho))*exp(sigma_G/Type(2.0));

for(int a=1;a<nages;a++) {
    Mean_logN_L(a) = (Type(1.0)-
pow(Rho,a))*log(Linf)+pow(Rho,a)*(log(mu_r)-
Type(0.5)*(sig2_r/pow(mu_r,Type(2.0))));
    Var_logN_L(a) =
pow(Rho,Type(2.0)*(a))*(sig2_r/pow(mu_r,Type(2.0)))+sigma_G*
((Type(1.0)-pow(Rho,(Type(2.0)*(a))))/(Type(1.0)-
pow(Rho,Type(2.0))));
};
for(int a=1;a<nages;a++) {
    SS(a) = exp(Type(2.0)*(Mean_logN_L(a)+Var_logN_L(a)))-
exp(Type(2.0)*Mean_logN_L(a)+Var_logN_L(a));
};

for(int a=1;a<nages;a++) {
    for(int xind=0;xind<nlengths;xind++) {
        kkk = Type(0.0); // normalizing constant;
        for(int Lind=0;Lind<nlengths;Lind++) {
            pp(Lind,xind,a) = Type(0.0);
            if(Lind >= xind) {
                pp(Lind,xind,a) = dnorm(L(Lind),Mu(xind),sqrt(SS(a)));

                kkk += pp(Lind,xind,a);
            };
        };
        for(int Lind=0;Lind<nlengths;Lind++)
            pp(Lind,xind,a) /= kkk;
    };
};
};

```

```

//std::cout << " !! GROWTH PROCESS FINISH !! " << std::endl;

// Abundance;
N.setZero();
NL.setZero();
Nx.setZero();
N_plus.setZero();
F_N.setZero();
F_NL.setZero();
M_N.setZero();
M_NL.setZero();
Spawners.setZero();
SpawnersL.setZero();
Sex_A.setZero();
ARRIVE.setZero();
Eggs.setZero();
F_f.setZero();
M_f.setZero();
F_f_init.setZero();
M_f_init.setZero();

ARRIVE(nages-2) = Pi_5;
ARRIVE(nages-1) = Type(1.0);

// Initial time, length frequency;
F_f_init.row(0) = f.row(0);
M_f_init.row(0) = f.row(0);
Sex_A_init(0) = Sex_r_female;

for(int a=1; a<nages; a++) {
    for(int Lind=0; Lind<nlengths; Lind++)
        for(int xind=0; xind<nlengths; xind++) {
            F_f_init(a,Lind) += F_f_init(a-1,xind)*(Type(1.0)-
ARRIVE(a-1)*maturation(xind))*pp(Lind,xind,a);
            M_f_init(a,Lind) += M_f_init(a-1,xind)*(Type(1.0)-
maturation(xind))*pp(Lind,xind,a);
        }
    }

```

```

    };
    Sex_A_init(a) =
    F_f_init.row(a).sum()/(F_f_init.row(a).sum()+M_f_init.row(a).sum(
));
    };
    for(int a=0; a<nages; a++) {
        F_f_init.row(a) = F_f_init.row(a)/(F_f_init.row(a).sum());
        M_f_init.row(a) = M_f_init.row(a)/(M_f_init.row(a).sum());
    };

    // Imaginary age structure;
    int a;
    for(int m=0; m<=nmos; m++) {
        if(m == 0) {
            for(int a=0; a<nages; a++) {
                for(int xind=0; xind<nlengths; xind++) {
                    F_NL(m,xind,a) =
                    N_init(a)*F_f_init(a,xind)*Sex_A_init(a);
                    M_NL(m,xind,a) =
                    N_init(a)*M_f_init(a,xind)*(Type(1.0)-Sex_A_init(a));

                    NL(m,xind,a) = F_NL(m,xind,a)+M_NL(m,xind,a);
                    SpawnersL(m,xind,a) =
                    F_NL(m,xind,a)*ARRIVE(a)*maturation(xind);
                    Spawners(a,m) += SpawnersL(m,xind,a);

                    F_N(a,m) += F_NL(m,xind,a);
                    M_N(a,m) += M_NL(m,xind,a);
                    N(a,m) += NL(m,xind,a);
                    Nx(m,xind) += NL(m,xind,a);
                };
            };
        } else if(m > 0) {
            a=0;
            for(int xind=0;xind<nlengths;xind++)
                for(int aa=0;aa<nages;aa++)

```

```

        Eggs(m-1)          +=          SpawnersL(m-
1,xind,aa)*fecundity(xind);

        N(a,m) = Eggs(m-1)*exp(-Type(1.0)*M(0)); //Eggs;
        for(int xind=0;xind<nlengths;xind++) {
            F_NL(m,xind,a) = N(a,m)*Sex_r_female*f(a,xind);
            M_NL(m,xind,a)      =      N(a,m)*(Type(1.0)-
Sex_r_female)*f(a,xind);
            NL(m,xind,a) = N(a,m)*f(a,xind);

            F_N(a,m) += F_NL(m,xind,a);
            M_N(a,m) += M_NL(m,xind,a);
            Nx(m,xind) += NL(m,xind,a);
        };
        Sex_A(a,m) = F_N(a,m)/N(a,m);
        for(int a=1;a<nages;a++) {
            for(int Lind=0;Lind<nlengths;Lind++) {
                F_p(Lind) = Type(0.0);
                M_p(Lind) = Type(0.0);
                for(int xind=0;xind<nlengths;xind++) {
                    F_p(Lind) += F_f(a-1,xind)*(Type(1.0)-ARRIVE(a-
1)*maturation(xind))*ExpZ(m-1,xind)*pp(Lind,xind,a);
                    M_p(Lind)      +=      M_f(a-1,xind)*(Type(1.0)-
maturation(xind))*ExpZ(m-1,xind)*pp(Lind,xind,a);
                };
            };
            if(a!=nages-1) {
                for(int Lind=0;Lind<nlengths;Lind++) {
                    NL(m,Lind,a) = Type(0.0);
                    F_NL(m,Lind,a) = Type(0.0);
                    M_NL(m,Lind,a) = Type(0.0);

                    F_NL(m,Lind,a) = F_N(a-1,m-1)*F_p(Lind);
                    M_NL(m,Lind,a) = M_N(a-1,m-1)*M_p(Lind);
                    NL(m,Lind,a) = F_NL(m,Lind,a)+M_NL(m,Lind,a);
                };
            };
        };
    };
}

```

```

    N(a,m) += NL(m,Lind,a);
    F_N(a,m) += F_NL(m,Lind,a);
    M_N(a,m) += M_NL(m,Lind,a);
    Nx(m,Lind) += NL(m,Lind,a);
};
Sex_A(a,m) = F_N(a,m)/N(a,m);
} else if(a == nages-1) {
    Spawners(a-1,m) = Type(0.0);
    for(int Lind=0;Lind<nlengths;Lind++) {
        SpawnersL(m,Lind,a-1) = Type(0.0);
        SpawnersL(m,Lind,a-1) = F_NL(m,Lind,a-
1)*ARRIVE(a-1)*maturation(Lind);

        Spawners(a-1,m) += SpawnersL(m,Lind,a-1);
    };
    for(int xind=0;xind<nlengths;xind++) {
        F_f(a,xind) = Type(0.0);
        M_f(a,xind) = Type(0.0);
        f(a,xind) = Type(0.0);
    };
    for(int xind=0;xind<nlengths;xind++) {
        F_f(a,xind) = F_f(a-1,xind)*ExpZ(m-
1,xind)*(Type(1.0)-ARRIVE(a-1)*maturation(xind)); // Note that!!
f(a,xind) in left term is length distribution of age (a-1==nages-1) at
the 'end' of time (m-1);
        M_f(a,xind) = M_f(a-1,xind)*ExpZ(m-
1,xind)*(Type(1.0)-maturation(xind)); // Note that!! f(a,xind) in left
term is length distribution of age (a-1==nages-1) at the 'end' of time
(m-1);
    };
    for(int Lind=0;Lind<nlengths;Lind++) {
        F_p(Lind) = Type(0.0);
        M_p(Lind) = Type(0.0);
        for(int xind=0;xind<nlengths;xind++) {
            F_p(Lind) += F_f(a,xind)*pp(Lind,xind,a); // Note
that!! f(a,xind) in right term is length distribution of age (a-

```

```

1==nages-1) at the 'end' of time (m-1);
        M_p(Lind) += M_f(a,xind)*pp(Lind,xind,a); //
Note that!! f(a,xind) in right term is length distribution of age (a-
1==nages-1) at the 'end' of time (m-1);
    };
};
F_N(a,m) = Type(0.0);
M_N(a,m) = Type(0.0);
Sex_A(a,m) = Type(0.0);
Spawners(a,m) = Type(0.0);
for(int Lind=0;Lind<nlengths;Lind++) {
    NL(m,Lind,a) = Type(0.0);
    F_NL(m,Lind,a) = Type(0.0);
    M_NL(m,Lind,a) = Type(0.0);
    SpawnersL(m,Lind,a) = Type(0.0);
    F_NL(m,Lind,a) = F_N(a-1,m-1)*F_p(Lind);
    M_NL(m,Lind,a) = M_N(a-1,m-1)*M_p(Lind);

    NL(m,Lind,a) = F_NL(m,Lind,a)+M_NL(m,Lind,a);

    if(Plus_switch == 1) {
        for(int xind=0;xind<nlengths;xind++) {
            F_NL(m,Lind,a) += F_NL(m-1,Lind,a)*ExpZ(m-
1,xind)*(Type(1.0)-ARRIVE(a)*maturation(xind))*pp(Lind,xind,a);
            M_NL(m,Lind,a) += M_NL(m-
1,Lind,a)*ExpZ(m-1,xind)*(Type(1.0)-
maturation(xind))*pp(Lind,xind,a);
            NL(m,Lind,a) += (F_NL(m-1,Lind,a)*(Type(1.0)-
ARRIVE(a)*maturation(xind))+M_NL(m-1,Lind,a)*(Type(1.0)-
maturation(xind)))*ExpZ(m-1,xind)*pp(Lind,xind,a);
            N_plus(m) += (F_NL(m-1,Lind,a)*(Type(1.0)-
ARRIVE(a)*maturation(xind))+M_NL(m-1,Lind,a)*(Type(1.0)-
maturation(xind)))*ExpZ(m-1,xind)*pp(Lind,xind,a);
        };
    };
};
F_N(a,m) += F_NL(m,Lind,a);

```

```

        M_N(a,m) += M_NL(m,Lind,a);
        N(a,m) += NL(m,Lind,a);
        Nx(m,Lind) += NL(m,Lind,a);
        SpawnersL(m,Lind,a)
F_NL(m,Lind,a)*ARRIVE(a)*maturation(Lind);
        Spawners(a,m) += SpawnersL(m,Lind,a);
    };
};
};
};
for(int a=0;a<nages;a++) {
    for(int xind=0;xind<nlengths;xind++) {
        f(a,xind) = NL(m,xind,a)/N(a,m);
        F_f(a,xind) = F_NL(m,xind,a)/F_N(a,m);
        M_f(a,xind) = M_NL(m,xind,a)/M_N(a,m);
    };
    Sex_A(a,m) = F_N(a,m)/N(a,m);
};
};
// Projection;
Eggs(nmos) = Type(0.0);
for(int Lind=0;Lind<nlengths;Lind++) {
    for(int a=0;a<nages;a++) {
        Eggs(nmos) += SpawnersL(nmos,Lind,a)*fecundity(Lind);
    };
};
N(0,nmos+1) = Eggs(nmos)*exp(-1.0*M(0));

//std::cout << " !! IMAGINARY AGE STRUCTURE FINISH !! "<<
std::endl;

// Catch & Yield & Biomass;
Pop.setZero();

```

```

B.setZero();
JIG_Catch.setZero();
JIG_Yieldhat.setZero();
PS_Catch.setZero();
PS_Yieldhat.setZero();
TO_Catch.setZero();
TO_Yieldhat.setZero();

for(int m=0;m<nmos;m++)
  for(int xind=0;xind<nlengths;xind++) {
    JIG_Catch(m,xind) =
Nx(m,xind)*(JIG_F_tx(m,xind)/Z(m,xind))*(Type(1.0)-
ExpZ(m,xind));
    PS_Catch(m,xind) =
Nx(m,xind)*(PS_F_tx(m,xind)/Z(m,xind))*(Type(1.0)-
ExpZ(m,xind));
    TO_Catch(m,xind) =
Nx(m,xind)*(TO_F_tx(m,xind)/Z(m,xind))*(Type(1.0)-
ExpZ(m,xind));

    JIG_Yieldhat(m) += JIG_Catch(m,xind)*Wt(xind);
    PS_Yieldhat(m) += PS_Catch(m,xind)*Wt(xind);
    TO_Yieldhat(m) += TO_Catch(m,xind)*Wt(xind);

    if(m < nmos-1) {
      B(m) += Nx(m,xind)*Wt(xind);
      Pop(m) += Nx(m,xind);
    } else if(m == nmos-1) {
      B(m) += Nx(m,xind)*Wt(xind);
      Pop(m) += Nx(m,xind);

      B(nmos) += Nx(nmos,xind)*Wt(xind);
      Pop(nmos) += Nx(nmos,xind);
    }
  };
};

```

```

JIG_SamSize.setZero();
PS_SamSize.setZero();
for(int m=0;m<nmos;m++)
    for(int xind=0;xind<nlengths;xind++) {
        JIG_SamSize(m) += JIG_length_compo(m,xind);
        PS_SamSize(m) += PS_length_compo(m,xind);
    };

for(int m=0;m<nmos;m++) {
    for(int xind=0;xind<nlengths;xind++) {
        JIG_LF(m,xind) =
(JIG_Catch(m,xind)/JIG_Catch.row(m).sum())*JIG_SamSize(m);
        if(PS_effort(m) != Type(0.0)) {
            PS_LF(m,xind) =
(PS_Catch(m,xind)/PS_Catch.row(m).sum())*PS_SamSize(m);
        } else {
            PS_LF(m,xind) = Type(1.0);
        };
    };
};
//std::cout << " !! CATCH FINISH !! " << std::endl;

// Objective function;
nll.setZero();
RSS.setZero();

// part1. Length composition ~ multinomial;
for(int m=0;m<nmos;m++) {
    vector<Type> Data_length_JIG = JIG_length_compo.row(m);
    vector<Type> Prob_length_JIG =
JIG_Catch.row(m)/JIG_Catch.row(m).sum();

    nll(0) -= Wighting_para(0)*dmultinom(Data_length_JIG,
Prob_length_JIG, true);

    if(PS_effort(m) != Type(0.0)) {

```

```

        vector<Type>          Data_length_PS          =
PS_length_compo.row(m);
        vector<Type>          Prob_length_PS          =
PS_Catch.row(m)/PS_Catch.row(m).sum();

        nll(1) -= Wighting_para(1)*dmultinom(Data_length_PS,
Prob_length_PS, true);
    };
};

for(int m=0;m<nmos;m++) {
    for(int xind=0;xind<nlengths;xind++) {
        RSS(0) += square(JIG_length_compo(m,xind) -
JIG_LF(m,xind));
        RSS(1) += square(PS_length_compo(m,xind) -
PS_LF(m,xind));
    };
};

// part2. Yield ~ lognormal;
vector<Type> elem_obj_JIG(nmos);
vector<Type> elem_obj_PS(nmos);
vector<Type> elem_obj_TO(nmos);
Type sig2_JIG_Y = Type(0.0);
Type sig2_PS_Y = Type(0.0);
Type sig2_TO_Y = Type(0.0);
elem_obj_JIG.setZero();
elem_obj_PS.setZero();
elem_obj_TO.setZero();

for(int m=0;m<nmos;m++) {
    elem_obj_JIG(m) = log(JIG_yield(m))-
log(JIG_Yieldhat(m)/Type(1000));
    if(PS_effort(m) != Type(0.0)) {
        elem_obj_PS(m) = log(PS_yield(m))-
log(PS_Yieldhat(m)/Type(1000));
    }
}

```

```

};
elem_obj_TO(m) = log(TO_yield(m))-
log(TO_Yieldhat(m)/Type(1000));
};
for(int m=0;m<nmos;m++){
sig2_JIG_Y += elem_obj_JIG(m)*elem_obj_JIG(m);
sig2_PS_Y += elem_obj_PS(m)*elem_obj_PS(m);
sig2_TO_Y += elem_obj_TO(m)*elem_obj_TO(m);
};

RSS(2) = sig2_JIG_Y;
RSS(3) = sig2_PS_Y;
RSS(4) = sig2_TO_Y;
sig2_JIG_Y /= nmos;
sig2_PS_Y /= (nmos-1);
sig2_TO_Y /= nmos;

for(int m=0;m<nmos;m++){
nll(2) -=
dnorm(log(JIG_yield(m)),log(JIG_Yieldhat(m)/Type(1000)),sqrt(log
(Type(1.0)+Wighting_para(2)*Wighting_para(2))), true);
if(PS_effort(m) != Type(0.0)) {
nll(3) -=
dnorm(log(PS_yield(m)),log(PS_Yieldhat(m)/Type(1000)),sqrt(log
(Type(1.0)+Wighting_para(3)*Wighting_para(3))), true);
};
nll(4) -=
dnorm(log(TO_yield(m)),log(TO_Yieldhat(m)/Type(1000)),sqrt(log
(Type(1.0)+Wighting_para(4)*Wighting_para(4))), true);
};

// part3. Weight ~ normal;
vector<Type> E_W = aWL*pow(lengthAL,bWL);
Type sig2AL = ((weightAL-E_W)*(weightAL-E_W)).sum()/nAL;
for(int i=0;i<nAL;i++){
nll(5) -=

```

```

Wighting_para(5)*dnorm(weightAL(i),aWL*pow(lengthAL(i),bWL),
sqrt(sig2AL),true);
};
RSS(5) = ((weightAL-E_W)*(weightAL-E_W)).sum();

// part4. Fecundity ~ lognormal: Not Used;
vector<Type> E_log_FC = log(aFC)+bFC*log(lengthFC);
vector<Type> E_FC = aFC*pow(lengthFC,bFC);
for(int i=0;i<nFC;i++) {
    if( Wighting_para(6) != 0) {
        nll(6) -=
Type(0.0)*dnorm(log(EggFC(i)),E_log_FC(i),sqrt(log(Type(1.0)+
Wighting_para(6)*Wighting_para(6))),true);
    };
};
RSS(6) = Type(0.0)*((log(EggFC)-E_log_FC)*(log(EggFC)-
E_log_FC)).sum();

// part 7. penalty term;
for(int i=0;i<(nmos-1);i++) {
    if(Wighting_para(7) != 0) { // if Likelihood_weight(7) is equals
to '0', penalized likelihood is not used;
        if(i == 0) {
            nll(7) -= dnorm(log_F_TO(i), log_TO_F_init,
sqrt(log(Type(1.0)+Wighting_para(7)*Wighting_para(7))));
        } else {
            nll(7) -= dnorm(log_F_TO(i), log_F_TO(i-1),
sqrt(log(Type(1.0)+Wighting_para(7)*Wighting_para(7))));
        };
    };
};

Type jnll=nll.sum(); // jnll: Joint Negative Log-Likelihood;

// REPORT SECTION;
REPORT(nll);

```

REPORT(ExpZ);
REPORT(Z);
REPORT(E_W);
REPORT(E_FC);
REPORT(JIG_Yieldhat);
REPORT(JIG_Catch);
REPORT(PS_Yieldhat);
REPORT(PS_Catch);
REPORT(TO_Yieldhat);
REPORT(TO_Catch);
REPORT(JIG_LF);
REPORT(PS_LF);
REPORT(JIG_length_compo);
REPORT(PS_length_compo);
REPORT(N);
REPORT(F_N);
REPORT(M_N);
REPORT(NL);
REPORT(F_NL);
REPORT(M_NL);
REPORT(maturation);
REPORT(Nx);
REPORT(M);
REPORT(B);
REPORT(JIG_F);
REPORT(PS_F);
REPORT(TO_F);
REPORT(JIG_F_tx);
REPORT(PS_F_tx);
REPORT(TO_F_tx);
REPORT(Sex_A);
REPORT(JIG_SamSize);
REPORT(PS_SamSize);
REPORT(SpawnersL);
REPORT(Spawners);
REPORT(Eggs);

```
REPORT(nlengths);
REPORT(Wighting_para);
REPORT(JIG_Sel);
REPORT(PS_Sel);
REPORT(TO_Sel);
REPORT(pp);
REPORT(f);
REPORT(F_f);
REPORT(M_f);
REPORT(SS);
REPORT(Mu);
REPORT(N_plus);
REPORT(jnll);
REPORT(sig2_JIG_Y);
REPORT(sig2_PS_Y);
REPORT(sig2_TO_Y);
REPORT(RSS);

return jnll;
}
```

